Mechanism of DNA Chemical Denaturation

Daniel Ostrovsky*,†,‡ and Mikhail V. Ostrovsky*,†,¶

†*Independent Researcher*

‡*ORCID ID: 0009-0002-8680-7499*

¶*ORICD ID: 0009-0006-4064-8727*

E-mail: dan.ostrovsky85@gmail.com; mvo2001@hotmail.com

Abstract

We develop the theory of chemical denaturation of DNA for low and medium denaturation degrees, including but not limited to 50% denaturation as a reversible first-order reaction. We show the degree of influence of hydrogen bonding, dispersion, polar forces, proton donor/acceptor ratio, dipole induction, orientation parameter, and electrostatic interaction on the denaturation process of DNA. The absolute enthalpy values for DNA chemical denaturation are significantly lower than in the thermal denaturation process (positive). We show that the mechanism of reaching 50% DNA denaturation thermally and chemically differs. The thermal denaturation process mainly involves breaking hydrogen bonds via heating DNA, while the chemical denaturation process involves replacing DNA hydrogen bonding with denaturants. We also show that hydrogen bonding is the most significant part of the enthalpy of chemical denaturation for T4 bacteriophage DNA, and the proton-donor effect is the dominant mechanism in disrupting hydrogen bonds in DNA denaturation. The influence of this effect is two times larger than the influence of the proton-acceptor effect. Another essential factor for DNA denaturation is the orientational component, part of the polar cohesion parameter. We suggested that the total cohesion parameter measured at 50% of DNA

chemical denaturation represents the electrostatic (repulsion) forces maintaining the DNA helix.

We demonstrate that theoretical and prior experimental results show that the Hildebrand, Hansen, Karger, Snyder, and Eon equations are applicable and instrumental in studying DNA chemical denaturation. We developed a novel method to reveal and estimate the degree of influence of electrostatic repulsion and different attraction forces in DNA during its chemical denaturation. Our method can be suitable for selecting DNA (or other systems with controllable denaturation) targeted for specific applications.

1. Introduction

DNA denaturation

A DNA duplex is a double-stranded helix generally maintained by hydrogen bonding between the two strands of DNA. It is defined by the nucleotide pairings A-T and C-G. The term denaturation for DNA means the loss of bonding between nucleic acid pairs due to the addition of solvent(s) or an increase in temperature. Each factor leads to the separation of double-stranded helical nucleic acids into single-stranded coils.

DNA denaturation plays an essential role in many biological processes. Understanding DNA denaturation is vital for understanding fundamental genetic processes such as replication and transcription. Other important applications for DNA denaturation are bioanalytical methods and molecular diagnostics. One such method is PCR (polymerase chain reaction), where the controlled denaturation/renaturation of DNA is a critical step in the process.

DNA denaturation is also important for many other practical applications such as gel electrophoresis, denaturing gradient gel electrophoresis, and sequencing by denaturation.[1] There are also some new directions for using partially or completely denatured DNA. Namely, it is becoming important for nanotechnology,[2–4] creating nanodevices,[5] medical applications such as new drug delivery systems,[6] studying drug-DNA interactions,[7] analyzing forensic

evidence,[8] making functional DNA sensors including metal sensing,[9] and designing molecular memories.[10] These techniques are based on the hybridization process for complementary nucleic acid strands. This process involves the denaturation and subsequent renaturation of DNA.[9]

Thus, studying DNA denaturation is essential not only for improving our knowledge of biological processes, advancing bioanalytical techniques, and improving molecular diagnostic methods but also for other medical applications, forensic evidence, DNA-based sensors, and nanodevice-related applications.

The rate and degree of the denaturation process depends on the following interrelated parameters:[11,12] temperature, structure and size of DNA, the composition of surrounding media (solvents,[13,14] buffers,[15] PH, salts,[16],[17 18]). Many theoretical and experimental works have been published to describe factors related to DNA denaturation. However, the precise mechanism of DNA denaturation is still poorly understood and has continued to attract the attention of researchers.[19]

The works where significant attention has been related to the creation of the theory we conditionally call the "theoretical work" and the studies where the major emphasis was placed on the experiment we conditionally call the "experimental work." We discuss both approaches below:

1.1 The theoretical works related to thermal denaturation of DNA without solvents.

The first well-known theoretical work on DNA denaturation by heating (without solvents) called the Poland–Scheraga model,[20,21] discussed by C.Richard and A.Guttmann.[22] According to the authors: *"The question of the mechanisms applied to real DNA responsible for the denaturation process and which explain behavior as observed in melting curves is still far from being satisfactorily answered."* The efforts toward improvement and further development or simplification of this model continue.[23–25]

Another rapidly developing direction of theoretical work toward understanding the denaturation process is the Nearest-Neighbor method, where the DNA helix is treated by the interaction between neighboring DNA/DNA base pairs.[26] I. Tinoco, O.Uhlenbeck, M. Levine[27] calculated thermodynamic parameters for the nearest neighbor sequence in DNA, J. Ir. SantaLucia, D. Hicks[26,28] and N. Sugimoto et al.[29] Sugimoto presented results of measurements of the DNA/DNA nearest-neighbor thermodynamic parameters of 50 DNA/DNA duplexes. J. Jr. SantaLucia and D. Hicks[28] developed a set of thermodynamic parameters describing DNA secondary structure. The authors[28] presented a thermodynamic parameters database for nearest neighbor base pairs needed to create programming algorithms to predict DNA secondary structures such as hairpins, internal loops, and mismatches. Based on this knowledge, J.Jr.SantaLucia created DNA software.

All these calculations were performed assuming that the enthalpy and the entropy of denaturation are independent of temperature. However, J. Petruska and M. Goodman[30] analyzed published experimental data for detachment of nearest neighbor doublets in DNA and found that the enthalpy of denaturation linearly depends on DNA melting temperature T_m in contrast to the conventional Gibbs relationship at equilibrium $\Delta H = T_m \Delta S$. A. Dragan, P. Privalov and C. Crane-Robinson showed experimentally,[31–33] that the enthalpy and entropy of DNA denaturation (ΔH, and ΔS) are linearly dependent on temperature. These authors[33] showed that previous calculations of the thermodynamic parameters (ΔH, and T_m) by the nearest-neighbor method must be corrected for the temperature dependence of the enthalpy of denaturation. A. Dragan et al. developed such a temperature correcting protocol. They compared ΔH and melting temperatures using the nearest-neighbor method with and without temperature correction with direct experimental data for different DNA duplexes. The results of such comparison show that T_m value perfectly matches the direct experimental data, but theoretically calculated ΔH values are lower than the experimental enthalpy values.[33]

Another important conclusion from A.Dragan, C.Crane-Robinson, and P. Privalov's

work[33] is that hydrogen bonds between DNA base pairs have a completely entropic nature and these bonds are responsible for 40% of Gibbs free energy. Van der Waals forces of enthalpic origin provide the remaining 60 % of Gibbs free energy.

Y. Kafri, D. Mukamel, and L. Peliti[34] studied the thermal denaturation of DNA using statistical mechanics for interacting and non-interacting loops. In this paper,,[34] the Poland–Scheraga model of DNA denaturation is extended to analyze loop formation and their interaction within the molecule. This analysis has been combined with the scaling theory for polymer networks. The authors conclude that the model exhibits critical behavior in some of its properties, such as the loop size distribution and the length of the segment. The model was extended to study the unzipping transition (denaturation) induced by an external force.

D. Marenduzzo et al. studied the dynamical scaling of the DNA denaturation (unzipping transition).[35] The authors theoretically compared DNA force-induced and thermal denaturation. The denaturation/unzipping dynamics on the phase boundary in the presence of a force are distinctly different from the thermal denaturation at zero force.

R.Wartell and A.Benight[36] created a theoretical model for DNA's thermal denaturation (helix-coil transition) and compared the theory with experimental results. The comparison of theory with experiment (melting curves for short segment DNAs) indicates that the base pair sequence has a relatively small influence on the stacking free energy. The agreement between theory and experiment is obtained for equilibrium transitions of 14 out of 15 fragments 80–587 bp (base pairs) long. The deviation between theory and experiment for a 516 bp DNA can be attributed to the formation of stem-loop structures. The explanation of inconsistent results observed with long DNA fragments was also attributed to the possible formation of loops.

Several models have been presented to predict DNA melting temperature T_m and to evaluate the influence of the factors describing T_m such as the length of DNA,[11,37,38] (T_m decreases for shorter pieces), sequence of nucleotide composition,[39–41] addition of salts (ionic strength, PH),[40–42] and influence of solvents.

1.2 Theoretical works related to thermal denaturation of DNA in solvent(s) presence

O.Sinanoglu and S.Abdulnur[43] show that the DNA double helix is stable in water but becomes denatured in some solvents. To reveal the role of water in keeping the helix together, the solvent contributions to the free energy difference between single strands and the helix are calculated for water, methyl alcohol, glycol, formamide, glycerol, ethanol, n-propanol, and n-butanol. The solvent's property crucial to denaturation is found to be mainly the enthalpy part of surface tension. Discussing the entropy contribution to the Gibbs free energy, the authors conclude that base (DNA) dipole orientation affects the solvent dipoles. They found that this effect depends on the dielectric constant change with temperature.

D. Macedo, I. Guedes, and E. Albuquerque[44] study solvent interaction effects on a DNA segment's nonlinear dynamical structure by using a time-independent perturbation approach. The authors investigated the denaturation temperature profiles and found that DNA's melting temperature decreases as the solvent potential increases.

Chi H. Mak[45] studied base stacking driving forces in DNA. He carried out large-scale molecular simulations to reveal the thermodynamic parameters (driving forces) behind the stacking interaction in DNA. To calculate the stacking free energy or Gibbs free energy, the author used the Monte Carlo calculation method and simulated purine and pyrimidine bases surrounded by many solvent molecules within a cubic box of up to 134 cubic angstroms in size. The author studied thermodynamic driving forces and physicochemical origins behind DNA-solvents stacking interaction. The computer simulation leads the author[45] to conclude that the solvent's entropy of hydrophilic origin is the major driving force for base stacking. At the same time, DNA backbone conformational entropy leads to the destabilization of base stacking. These two opposite entropic effects almost compensate for each other, producing a mild total stacking-free energy of around one kcal/mol. Another conclusion of the author[45] is that hydrogen bonding, charge-charge interaction, and dispersive forces have a small influence on DNA stability.

1.3 Experimental works.

A significant number of experimental works have been performed in the last fifty years,[46],[47],[48],[49],[50],[14] studying the role of chemicals (solvents) in DNA melting.

The articles in this section are subdivided into the following subgroups:

1. DNA thermal denaturation without solvents,

2. DNA denaturation by solvents at constant temperature.

3. Thermal denaturation in the presence of solvents

The second group we will call "chemical denaturation," and the third group will be defined as mixed thermal and chemical denaturation. The third group includes experimental works studying the influence of solvents on DNA denaturation at different temperatures or, if the temperature-dependent testing method has been used, even at a slow increase in heating rate.

1.3.1 Thermal denaturation without solvents.

Yakovchuk et al.,[51] and Privalov[52] studied the role of base-stacking and base-pairing contribution to the thermal stability DNA using calorimetry (spectrophotometer) and gel electrophoresis. Discussing the role of hydrogen bonding between conjugate base pairs, authors[52,53] concluded that the formation of hydrogen bonds is an entropy-driven, non-enthalpic process. The disruption of the Van der Waals contacts between base pairs explained large enthalpy values during DNA melting. The authors explained it by a disruption of apolar contacts between bases. This means that a significant part of the DNA denaturation/renaturation's enthalpy is supposed to be allocated to dispersion forces.

Privalov[52] defines DNA renaturation as the sequence of the following interrelated steps: base pairing and base stacking. Both these processes required proper orientation of corresponding bases that were needed for the formation of hydrogen bonding.

1.3.2 Chemical denaturation.

L. Levine, J. Gordon, and W. Jenks[46] studied the chemical denaturation of T4 bacteriophage DNA at constant buffer composition and temperature in the presence of different denaturants. The authors mainly used the immunological method[54] that determines only denatured DNA. The authors found a critical concentration for each denaturant needed to create 50% DNA denaturation.

M Xu, T Dai, Y Wang, and G Yang[55] used UV spectrophotometry to study the denaturation of DNA with high and low molecular weight in the absence and presence of different concentrations of dimethyl sulfoxide (DMSO). They also analyzed changes in the configuration of DNA using atomic force microscopy (AFM technique) and dynamic light scattering (DLS). Each stage of AFM treatment of DNA samples was performed at a constant temperature, so this method of investigating the denaturation process has to be classified as the chemical, not the thermal type.

The images on AFM-tested mica slides show DNA denaturation regions. Quantitative analysis of the distinctly denatured areas on the slides was performed by imaging software, and using the worm-like-chain model allowed authors to reveal the dependence of DNA persistence length on the concentration of DMSO. Analysis of this data led authors[55] to conclude that the persistent length of DNA decreases with the addition of DMSO. A substantial decrease in persistent length (from 50 to 12 nm) occurs at the addition of only 3% DMSO to the solution, which is significantly below the DMSO concentration corresponding to the melting point. The addition of 1% DMSO leads to 11% denaturation of 5000bp DNA. The authors concluded that even low DMSO concentration leads to a partial breaking of hydrogen bonds and weakening of base stacking forces before the complete transition of ds-DNA to ssDNA. Results also show a change of configuration (increase in DNA compaction) if the concentration of DMSO rises from 0.1% to 1%.

L. Chen, Y.Wang, and G. Yang[56] studied partially denatured DNA compaction related to the change in conformation of DNA in the presence of DMSO and magnesium chloride

using AFM, Dynamic Light Scattering, and electrophoretic mobility methods. The authors show that adding DMSO and a divalent cation (magnesium) to the DNA-containing system leads to the compaction of DNA even at its partial (low) denaturation. Authors show that the compaction of DNA increases at low concentrations of magnesium chloride and decreases at its higher concentrations (with the same concentration of DMSO). The electrophoretic mobility of DNA particles shows nonlinear dependence with rising concentrations of magnesium chloride (curve with maximum). The authors explained some of these effects by the influence of ionic strength on the electrostatic repulsion of the segments of DNA with negatively charged phosphate groups. The change in the degree of denaturation accompanying these effects was not measured.

C Tongu, T Kenmotsu, Y Yoshikawa[57] studied shrinking of T4 DNA (166 kbp) samples by adding divalent and trivalent cations. DNA samples were again placed on a mica slide surface, incubated, and dried at room temperature. Then, the DNA on the mica slides was analyzed using AFM imaging with scanning probe microscopy at a constant temperature. Results show that divalent cations create shrinkage of DNA, but adding three-valent cations to a DNA solution containing two-valent cations inhibits this shrinkage.

1.3.3 Thermal denaturation in the presence of solvents.

B. Hammouda and D. Worcester[14,50] studied the thermal denaturation transition (T_m) of Salmon DNA in water and aqueous solutions of alcohols, ethylene glycol, and glycerol. The authors used UV light absorption spectroscopy with a slow heating rate and a 260nm line to control the melting of the helix. The authors also used small-angle neutron scattering. They showed that DNA melting temperatures depend on the nature and concentrations of the solvent, and the T_m value is different than in the case of denaturation in water. The authors explain the results of their experiments by the solvent's ability to cross the hydrophobic sugar-rich region in DNA that behaves like a cylindrical micelle.

G. Bonner and A. Klibanov,[58] using a similar (spectrophotometric) method, studied the

influence of different synthetic and natural DNA and different solvents (DMSO, glycerol, ethylene glycol) on DNA structure and stability. Their results show a significant shift in melting temperature (T_m) for all non-aqueous solvents compared to water. Also, the authors found an increase of T_m values for denaturation of synthetic duplex DNA (21-mer) with an elevation in the concentration of sodium chloride. In conclusion, the authors highlighted the importance of hydrophobic interactions of solvents with DNA during denaturation.

R.Blake and S.Delcourt,[59] show that the addition of formamide to DNA solution decreases DNA melting temperature by $2.4 - 2.96°C$ per mole of formamide depending on the (G+C) content in DNA composition.

Mura[15] studied the influence of different buffers on DNA denaturation. The study was carried out using phosphate, Tris, and citrate buffers at fixed pH 7.4 at concentrations varying systematically. They found that DNA stability increases with buffer concentration and is explicitly influenced by buffer type.

Sturtevant and Geyduschek[60] calorimetrically studied the influence of pH on the enthalpy of DNA denaturation. They conclude that the entire enthalpy change occurs in the narrow pH range associated with the macromolecular configuration change.

S. Nakano and N. Sugimoto presented a review[13] related to the structural stability of DNA and RNA in the presence of organic solvents. The authors discussed some possible mechanisms of the influence of organic solvents on nucleic acid interactions. Among these mechanisms are the influence of the osmotic pressure and the dielectric constant effects on specific interactions with nucleic acid strands.

The theoretical and experimental works cited above show the influence of several factors and parameters on DNA denaturation in the presence and absence of different solvents. However, the work will continue to develop an equation connecting the rate and degree of DNA denaturation with the following interrelated parameters: the structure and state of DNA, the composition of surrounding media (solvents, buffers, PH), and temperature. Such information helps to select the proper (co)solvent or predict the required structure and

concentration of an additive to a solution (buffer) sufficient for good DNA denaturation or double-stranded DNA stabilization at a given temperature.

The experimental works above are based on a limited number of selected denaturants and do not give sufficient information on how to extend the denaturant selection or how to predict the required structure and concentration of a denaturant sufficient for complete or (if needed) for just partial DNA denaturation. The theoretical publications quoted above describe different models with assumptions that limit their predictability for denaturant selection.

1.4 Cohesion (solubility) parameters

The cohesion or solubility parameter represents a substance's cohesive energy density or the energy needed to vaporize one mole of a substance and expand the vapor until molecules cannot interact. Cohesion or solubility parameter study and its practical applications in multiple areas of human activity[61,62] has attracted the attention of many scientists in the academy and industry[63–65] . Several published theoretical articles attempted to extend the predictability of Hansen parameters beyond the solubility of polymers[65] ,[66] . We found no attempts in the literature to find the relationship between the experimentally determined cohesion parameters (HSP) and DNA denaturation in different solvent/cosolvent compositions. One of the purposes of the present article is to find such a relationship. According to its definition, the cohesion parameter is part of the enthalpy of solubility processes and is used to find/define the boundary for solute-solvent solubility.

The following are major steps in theoretical development in this area. Hildebrand[67,68] introduced this parameter. Then Prausnitz, with co-workers,[69–71] split the parameter into two components related to the forces hidden in the enthalpy of a transition process. Hansen[63,72,73] further suggested using the three-component splitting of the cohesion parameter. Hansen defined the solubility parameter (HSP or HSPiP) as cohesive energy density, which keeps molecules together in a liquid or solid state. The HSP can be used to evaluate the relative

role of polar, non-polar(dispersion), and hydrogen cohesive forces in a chemical composition. Karger, Snyder, and Eon[74,75] developed a five-component set of cohesion parameters that included additional HSP physicochemical properties related to the enthalpy of a system, such as an orientation. The inclusion of this parameter is based on the Kirkwood-Frohlich theory,[76],[77] which discussed the influence of the orientation of the electric dipoles in polar liquids. The orientation effect, according to this theory, correlates with dielectric constant.[78] Work on modification of solubility parameters continues (see, for example,,[79][80]). Authors[79] suggested replacing cohesive energy densities with electrophilicity densities that incorporate the charge transfer effect as a critical contribution to the Hildebrand approach. No fractional cohesion parameters were proposed in this[79] approach. We will discuss the progress related to the transition from one to five-component cohesion parameters models in more detail below, particularly the application of some of these parameters for evaluating the DNA denaturation process.

Overall, we can conclude that extensive work has been published in the literature on DNA's thermal and combined thermal-chemical denaturation. However, additional work is needed to establish essential factors and their relationship to pure chemical DNA denaturation. To reveal and better understand the mechanism of these processes, we are using physicochemical concepts such as thermodynamics (see below).

2. Theory

2.1 Kinetic and thermodynamics of DNA denaturation

The complete denaturation of DNA with high molecular mass (full transition from double-stranded, DS, helical nucleic acids to single-stranded, SS coils or DNA "melting") is a two-stage reversible consecutive dissociation reaction. Intermediate partial denaturation (PD) is the first stage. This happens with the formation of forks and/or bubbles inside the DNA helical structure and/or coils created from the initial helix, which continue to be bound to

the initial helix. This first partial denaturation stage can be expressed as:

$$DS \Longleftrightarrow PD \Longleftrightarrow 2SS \tag{1}$$

In the case of short DNA, the intermediate step can be omitted, and the process can be expressed as a simple reversible dissociation reaction :

$$DS \Longleftrightarrow 2SS \tag{2}$$

The ratio of the rate constants for the forward and reverse processes K_a and K_b can be written as the equilibrium constant "K":

$$K = \frac{K_a}{K_b} \tag{3}$$

The equilibrium constant K for the initial step of dsDNA denaturation with the formation of partially denatured pdDNA, according to expression 1 , is equal to:

$$K = \frac{[PD]}{[DS]} \tag{4}$$

Here, $[DS]$ and $[PD]$ are the concentrations of double-stranded (helix) and denatured sections inside of each partially denatured DNA molecule. The number of DNA molecules in this stage of denaturation does not change. In this case, the equilibrium constant represents the degree of DNA denaturation.

The equilibrium constant K' for the final step of pdDNA denaturation with the formation of single-stranded DNA, $ssDNA$, according to expression 1, equal to:

$$K' = \frac{[SS]^2}{[PD]} \tag{5}$$

Here $[SS]$ is the concentration of single-stranded DNA.

The equilibrium constant K" for the denaturation of dsDNA with low molecular weight to direct formation of single-stranded DNA, $ssDNA$, according to expression 2, equal to:

$$K" = \frac{[SS]^2}{[DS]} \tag{6}$$

Combination of the equation for Gibbs free energy change:

$$\Delta G = \Delta H - T\Delta S \tag{7}$$

and the Gibbs free energy isotherm equation:

$$\Delta G = -RT \ln K \tag{8}$$

leads to the Van't Hoff or Arrhenius expression for the temperature dependence that can be applied to the degree of DNA denaturation:

$$\ln K = A - \frac{\Delta H}{RT} \tag{9}$$

Here ΔS is entropy change, T is the temperature in degrees Kelvin, ΔH is the transition enthalpy at temperature T, R is the universal gas constant, and $A = (\Delta S/R)$.

The DNA denaturation process can be activated either by heating (thermal denaturation) or by adding denaturant(s), co-solvent(s), or changing buffer (PH) in the system (chemical denaturation). The mechanisms of both processes are different.

The thermal denaturation of DNA involves heating DNA, leading to breaking bonds, specifically hydrogen bonds and hydrophobic stacking attractions between the bases. Thus, thermal denaturation is an endothermic process that absorbs heat, making the net enthalpy change positive, $\Delta H_{thermal} > 0$. Thermal denaturation has been proved to be endothermic by measurement of the temperature dependence of $\ln K$. (See, for example,[46]). Gibbs free energy change, in this case, is positive, $\Delta G > 0$.

All processes with $\Delta G > 0$, including DNA thermal denaturation, are not spontaneous.

The chemical denaturation process (at constant temperature) involves replacing the initial bonds that keep DNA in double-strand form with new "DNA + denaturant" bonds with higher energy of attraction than the previous hydrogen bonds. This leads to the separation of DNA strands and the formation of random coils or single-stranded states.

Thus, chemical denaturation is the exothermic process of releasing heat, making the total enthalpy change negative, ΔH <0.

Any process has to be spontaneous in the case of $\Delta G < 0$. According to equation 7, this condition takes place a) at all temperatures if $\Delta S > 0$, but b) in the case of $\Delta S < 0$. Spontaneous processes at $\Delta H < 0$ are possible only at very low T when the product $T\Delta S$ is small.

DNA chemical denaturation process is spontaneous (except the case "b" above) because:

$$\Delta H < 0; \Delta G < 0 \tag{10}$$

The chemical denaturation process in a liquid solution (with the enthalpy defined as ΔH_{chem}) has two consecutive stages. The first stage is endothermic (with ΔH_{endo}) when initial bonds in DNA are disrupted. The second stage is exothermic (with ΔH_{exo}) when the open, active sites of DNA molecules interact with molecules of surrounding media, forming new bonds or restoring previous bonding inside DNA (renaturation). These two sequential stages in the denaturation process with different signs for ΔH have their contribution to the total enthalpy of DNA denaturation ΔH_{chem}. The second stage cannot occur if the first stage does not occur. The total enthalpy of DNA denaturation in Eq. 9 in the case of two *consecutive* stages of this process can be treated as a sum of the enthalpies for both these stages

$$\Delta H_{chem} = \Delta H_{endo} + \Delta H_{exo} \tag{11}$$

and

$$\ln K = A - \frac{\Delta H_{endo} + \Delta H_{exo}}{RT} \tag{12}$$

Parameters $\Delta H_{thermal}$ and ΔH_{endo} are not necessarily equal. The experimental part of this paper will discuss a comparison of enthalpies of thermal and chemical denaturation processes.

Parameter A in Eq. 9 can be found at DNA melting temperature (Tm) when $\ln K = 0$:

$$A = \left(\frac{\Delta S}{R}\right)_{T=Tm} = \left(\frac{\Delta H}{RT}\right)_{T=Tm} \tag{13}$$

The melting temperature T_m is the temperature for 50 percent DNA denaturation. Here, a molecule of DNA is partially (50%) denatured. At such conditions, Equation 4 for a partially denatured state applies with [PD]= [DS] and K=1.

Equation 4 describes internal DNA denaturation without splitting single-stranded molecules from the initial or partially denatured DNA unit. The denaturation process leads to an internal conformational change in DNA, decreasing the [DS] fraction in each macromolecule and increasing the [PD] fraction.

Substitution of Eq. 13 to Eq. 9 with condition 10 gives an expression for the chemical denaturation process:

$$\ln K = \frac{\Delta H}{RT} - \left(\frac{\Delta H_{DNA}}{RT}\right)_{T=T_m} \tag{14}$$

The equation 14 shows that the degree of DNA denaturation (K) reflects the difference in the enthalpy inside double-stranded DNA at melting temperature and the enthalpy inside the denaturant/solvent mixture at the temperature of the experiment. Parameters ΔH and ΔH_{DNA} are not equal if the temperature of the experiment is not identical to T_m, but they become equal at $T = T_m$.

At melting temperature, the enthalpy change in the DNA molecule is equal to the enthalpy change of the surrounding solution:

$(\Delta H_{DNA})_{T_m} = \Delta H_{T_m}$.

Equation 14 shows that the denaturing ability of a denaturant that influenced the degree of DNA denaturation (K), is a function of the temperature of experiment, T, DNA melting temperature T_m, the total enthalpy (ΔH) of a solution at temperature of experiment and $(\Delta H)_{DNA}$ at melting temperature.

Combination of Eqs. 14 and 11 gives:

$$\ln K = \frac{\Delta H_{endo} + \Delta H_{exo}}{RT} - \left(\frac{\Delta H_{DNA}}{RT}\right)_{T=T_m} \tag{15}$$

and in the case $T = T_m$, when $\ln K = 0$ we have:

$$\Delta H_{chem,T_m} = \Delta H_{endo} + \Delta H_{exo,T_m} = \Delta H_{DNA,T_m} \tag{16}$$

Total enthalpy ΔH_{chem} for chemical denaturation will be calculated based on specific physicochemical parameters for the solutions of different chemicals used for DNA denaturation experiments at a constant temperature corresponding to DNA melting. We perform such calculations using cohesion or Hansen solubility parameters (HSP), which are discussed in the next section of this paper.

In the case of equilibrium $\Delta G = 0$, and equation 7 is simplified to:

$$T_m = \left(\frac{\Delta H}{\Delta S}\right)_{T=T_m} \tag{17}$$

According to this equation, the melting temperature in chemical or thermal denaturation processes (and in any energy exchange processes) equals the ratio of enthalpy and entropy changes at the melting temperature. Comparison of Eqs 17 and 14 shows that a single component containing the entropy term in the last of these two equations is T_m.

2.2 Relation between enthalpy and cohesion parameters for one solvent and the multi-component solutions of denaturants.

2.2 .1 DNA denaturation in one component liquid systems.

To find the enthalpies for the solutions with chemicals for DNA chemical denaturation, we applied the Hansen solubility parameters (HSP). We decided to use HSP because, for chemical denaturation, both the conduction of denaturation experiments and the measurement of the enthalpy for DNA denaturation have to be done at a constant temperature.

Hildebrand[68] considered the change in cohesive energy per unit volume (cohesive density):

$$C = -\frac{U}{V} \tag{18}$$

Here U is the molar internal energy; $-U$ is molar cohesive energy associated with net attractive interactions of the material, V is the molar volume where:

$$-U = \Delta H_1 + \Delta H_2 - RT + PsV'$$

Here ΔH_1 is the molar enthalpy of vaporization, ΔH_2 is the molar enthalpy for expansion of the saturated vapor to infinite volume. V' is the molar volume of the liquid being evaporated. At $T \ll T_{\text{boiling}}$ terms 2 and 4 can be neglected:

$$-U = (\Delta H_1 - RT) \tag{19}$$

A combination of equations 18 and 19 leads to the expression known as Hildebrand parameter[67] :

$$\delta = \sqrt{C} = \sqrt{\frac{\Delta H_1 - RT}{V}}$$

or to the expression for cohesive energy density:

$$\delta^2 = \frac{\Delta H_1 - RT}{V}$$

and to Hildebrand's equation:

$$\Delta H_1 = \delta^2 V + RT \tag{20}$$

Hildebrand parameter was confined to nonassociating and nonpolar systems, but the concept has been extended to the types of systems beyond these restrictions.

The values of δ (the Hildebrand parameter) are calculated using this equation with experimentally determined values of ΔH and the molar volume of a liquid V.

Comparison of equations 20 and 17 (which represents Eq.7 at equilibrium conditions) shows the difference in the thermodynamic concepts of Gibbs and Hildebrand. They divided total molar cohesive energy (enthalpy) into different segments. Gibbs defined the enthalpy as the product of the temperature and the entropic term ΔS. Hildebrand defined the enthalpy as the sum of RT and the temperature-independant term $\delta^2 V$. We combined both these approaches, namely, combine Eq. 9, (which is derived from Eq. 7), with Eq.20.

The right part of equation 20 is always positive, but the left part can be positive (the thermal DNA denaturation case) or negative (the chemical denaturation case). In the last case, Equation 20, with condition 10, leads to a modified Hildebrand equation related to the chemical type of DNA denaturation:

$$\Delta H_1 = -\delta^2 V - RT \tag{21}$$

Parameter $\delta^2 V$ is known as total *cohesion or solubility parameter.*[72]

According to Hansen,[72,73] cohesive energy is made up of a combination of additive contributions from fractional cohesion parameters called Hansen parameters

$$\delta^2 = \delta_d^2 + \delta_h^2 + \delta_p^2 \tag{22}$$

where δ_d^2 is the dispersion or non-polar cohesion parameter, δ_h^2 is the hydrogen bonding cohesion parameter, and δ_p^2 is the polar cohesion parameter. Methods for measuring and calculating these fractional parameters are described in[61] and.[72] Dimension of δ^2 is Joule/cm^3, V is cm^3/mole, $\delta^2 V$ and RT are Joule/mole.

Combination of equations 15, 16, and 21 (the case $\Delta H < 0$) gives:

$$\ln K = \frac{(\delta^2 V)_{sol}}{RT} - \left(\frac{(\delta^2 V)_{DNA}}{RT}\right)_{T_m} \tag{23}$$

In the case of constant $T = Tm$ and the same DNA in all denaturing experiments, $lnK = 0$ and expression 23 has a form:

$$(\delta^2 V)_{DNA,T_m} = (\delta^2 V)_{sol,T_m} \tag{24}$$

Subscript "sol" in these equations means a solution for denaturation. Parameter $[(\delta^2 V)_{sol}]$ equal according to Eq. 21 to the term $[-(\Delta H)_{chem} - RT]$.

Using equations 22 and 24, we know that at the melting temperature, the product of molar volume on each of the three fractional cohesion parameters is the same in the solution as well as in DNA.

$$[(\delta_d^2 + \delta_h^2 + \delta_p^2)V]_{DNA,Tm} = [(\delta_d^2 + \delta_h^2 + \delta_p^2)V]_{sol,Tm} \tag{25}$$

The modified Hildebrand parameter 21 applies to exothermic processes such as chemical denaturation.

2.2.2 DNA denaturation in multi-component liquid systems.

A liquid media for DNA or RNA denaturation is usually a blend of aqueous solvents/denaturant(s), salts, and a buffer. We considered such systems as the media for the chemical (exothermal) type of the denaturation process. Evaluation of the effective cohesion parameters $\overline{\delta}$ for liquid

mixture is of prime importance for selecting a proper mixture of solvents for the denaturation of nucleic acids. Hildebrand and Prausnitz[68] assumed in developing the expression for cohesion parameter that the value of effective parameter $\overline{\delta}$ for a solvent mixture is volume-wise proportional to the similar parameters of its components. We assumed similarly to[68] that for the multi-component solution, the additivity principle for enthalpy ΔH_i and volume fraction V_{f_i} for each component in the solution apply. See Assumption 1 below and compare it to equation 20.

Assumption 1. *We assumed that for the multi-component solutions, we can apply the additivity principle for enthalpy ΔH_i and Hansen parameter $\delta_i^2 V_i$ per volume fraction V_{f_i} of each component.*

$$\Delta H = \sum_{i=1}^{i=j} \Delta H_i V_{f_i} = -\left(\sum_{i=1}^{i=j} \delta_i^2 V_i V_{f_i} \right) - RT \tag{26}$$

Each $\Delta H_i, V_i$ and δ_i^2 values in Eq. 26 has identical property to corresponding pure component.
The sum of all volume fractions in the system equal to one:

$$\sum_{i=1}^{i=j} V_{f_i} = 1 \tag{27}$$

In addition to the thermodynamic approach, we need to consider the influence of the structural/sizing effect resulting from differences in molecular sizes for a denaturant, water, and other components in the solution. The corresponding sizing parameter we selected, V_r, is the ratio of the molar volume of a component V to the molar volume of water V_w:

$$V_r = \frac{V}{V_w} \tag{28}$$

An increase in the size of a denaturant molecule can decrease the rate constant for the denaturation process (K_1 for $DS \rightarrow SS$) and/or the rate constant (K_2) for the opposite, renaturation process ($SS \rightarrow DS$). The influence of the size of the denaturant's molecules on

K_1 and on K_2 can be different, and the total rate of denaturation $K = (K_1/K_2)$ can increase or decrease with the denaturant's size. From this, we can conclude that the selected geometric mean approximation $lnK = f(V_r)$ has two opposite scenarios $\frac{dlnK}{dV_r} < 0$ or $\frac{dlnK}{dV_r} > 0$. The first one can be described as $lnK = (Z/V_r)$. Here, Z is the coefficient explained in expression 30. The second scenario has a form:

$$lnK = (Z * V_r) \tag{29}$$

This is the first approximation of the influence of the size of the denaturant on denaturation. The last equation for the chemical type of DNA denaturation process has been validated in the experimental part of this paper. This approximation for the influence of the sizing effect of denaturants on the exothermal denaturation process comes from the experimental part of the paper.

Combining equations 23, 26 with 29 for the chemical type of denaturation in multicomponent systems, we have the following expression:

$$\ln K = V_r \left(\frac{\sum_{i=1}^{i=j} \delta_i^2 V_i V_{f_i}}{RT} \right)_{sol} - V_r \left(\frac{(\delta^2 V V_f)_{DNA}}{RT} \right)_{T_m} \tag{30}$$

where $(V * V_f)_{DNA,T_m}$ is the product of molar volume and volume fraction of DNA at melting temperature.

Based on equation 30, we have developed a method to estimate the type and required concentration of different denaturants to create a solution with perfect denaturing power. Such denaturant(s) should have a high value of the fractional Hansen solubility parameter related to the limiting enthalpic component needed for denaturation and have sufficient solubility in a targeted solvent/co-solvent mixture at the required temperature. For example, the composition selected for effective DNA chemical denaturation should have a high value of partial cohesion parameter δ_h related to hydrogen bonds.

In the case of constant $T = T_m$ and the same type and concentration of DNA in all

denaturing experiments $\ln K = 0$ and Equation 30 has a form:

$$\left(\delta^2 V V_f\right)_{DNA,T_m} = \left(\sum_{i=1}^{i=j} \delta_i^2 V_i V_{f_i}\right)_{sol,T_m} \tag{31}$$

The expression 31 shows that there is a matching interaction condition between DNA and other components in the solution. This allows us, for the case of $lnK = 0$, when the matching equilibrium between DNA and solution is established (Eq. 31), to determine the thermodynamic parameters of DNA by measuring these parameters of the surrounding solution.

We have developed a theory describing the chemical denaturation of DNA as a reversible first-order reaction. The theory links the degree of DNA denaturation with Hildebrand, Hansen, and KSE cohesion parameters, concentration (volume fraction) of a denaturant, and temperature.

3. Experimental Part

We analyzed published experimental data of other researchers using our theoretical framework to verify our theory. This is necessary for independent verification of our theory.

3.1 Materials and Methods

DNA and its denaturation.

The primary dataset of 31 chemicals for DNA denaturation was tested by.[46] The following DNA types have been tested:[46] T4 Bacteriophage, Diplococcus pneumoniae, B.subtilis, calf thymus, S. coli B, Serratia marcescens, Ps. aeruginosa and S. viridochromogenes. The majority of the experiments were done on the T4 Bacteriophage DNA at a concentration of $16\mu g/ml$ in a buffer containing 0.005 M Tris, and 10^{-3} M EDTA, pH 7.6, and incubated for 30 minutes at $73°C$. Then DNA samples were cooled rapidly on ice. Following DNA denaturation, an immunologic method was used to identify solely denatured DNA.[46] The

logarithmic plot of the ratio of denatured to native DNA against the concentration of denaturing agents was used to calculate the concentrations of denaturing agents needed to give 50% denaturation of DNA under these conditions. The thermal DNA denaturation has also been studied using immunological and optical (refractometry, relative absorbancy of $260m\mu$) methods. Experiments were performed[46] to study DNA denaturation as a function of DNA concentration ranging from $0.9\mu g/ml$ to $30\mu g/ml$. The present article provides new insight into experimental data cited above[46] by combining with effective cohesion parameters of solutions using a newly developed method below.

Method of calculation of physicochemical parameters for DNA chemical denaturation.

The method of calculation of the total and fractional enthalpies for DNA three-set cohesion parameters is presented in the form of equations 37, 38, 39, 40 and for five-set cohesion parameters as equations 42, 43, 44, 45, 46. The experimentally determined and published values of cohesion parameters for all tested denaturants and water were adapted from the references in Tables 1 and 4.

3.2 Verification of the theory: DNA denaturation analysis using Hansen cohesion parameters.

To verify the theory above, we analyzed published experimental data containing information needed for inclusion in Eqs. 31 and 30 and calculation of ΔH_{sol}.

Values of experimentally determined Hildebrand parameters δ and molar volumes V (at $25°C$) for denaturants shown in Table 1 have been adapted from literature,[61],[63],[81].[82] These data have been used to calculate enthalpies for each solution composition.

Note that the values of δ and V separately depend on temperature, but the function $\delta^2 V$ (Hansen solubility parameter, HSP) according to Eq. 20 is temperature independent. Thus, we can apply HSP calculated for $25°C$ to the actual experimental temperature for DNA denaturation.

Levine, Gordon, and Jencks's[46] studied at constant temperature ($73°C$) the effectiveness

of a broad spectrum of chemicals as denaturing agents (See Table 1). These authors show the dependence of the denaturation degree, K, for T_4 bacteriophage DNA from the concentration of denaturants M, expressed in Mol/l. They found the concentration for each additive M_{T_m} corresponding to 50 percent DNA denaturation that equals $K = 1$. These data are also presented in Table 1.

Based on recalculated data from,[46] we presented the dependence of lnK from the volume fraction of the denaturant V_f. (Fig 1). The data show that for each denaturant, there is a linear dependence between $\ln K$ and V_f. The following equation describes this:

$$\ln K = a + bV_f \tag{32}$$

Empirical equation 32 is similar to our theoretical expression 30 where a has a form:

$$a = V_r \frac{\left(\sum_{i=2}^{i=j} \delta_i^2 V_i V_{f_i}\right)_{sol}}{RT} - V_r \left(\frac{(\delta^2 V V_f)_{DNA}}{RT}\right)_{T_m} \tag{33}$$

and b is supposed to be equal to:

$$b = \frac{(\delta_1^2 V_1 V_{r_1})_{sol}}{RT} \tag{34}$$

where index 1 means a denaturant.

Our task is to verify our theory using experimental data (Fig 1) by comparing the slopes on graphical dependence lnK vs. V_f (b experimental) with theoretical b values from expression 34. Results show that experimental and theoretical values for "b" parameters are reasonably close to each other, except cyclohexanol (cyclic molecular structure). Our selection of structural parameter V_r needs correction to accommodate this deviation for cyclohexanol

Table 1:
Denaturant concentration (M) giving 50% denaturation of T4 Bacteriophage DNA in buffer solution at 73°C and Hansen parameters of denaturants at 25°C

#	Denaturants	M (*) Mol/Liter	V cm^3/mol	δ_d at 25 ° C	δ_h at 25 ° C	δ_p at 25 ° C	Total δ	Referral for Hansen data
	Alcohols							
1	Methyl alcohol	3.5	40.7	15.1	22.3	12.3	29.6	Ref. 61, pg 101.
2	Ethyl alcohol	1.2	58.5	15.8	19.4	8.8	26.5	Ref. 61, pg 101.
3	Isopropyl alcohol	0.9	76.8	15.8	16.4	6.1	23.5	Ref. 61, pg 101.
4	n-Propyl alcohol	0.54	75.2	16	17.4	6.8	24.5	Ref. 61, pg 101.
5	Allyl alcohol	**0.5**	68.4	16.2	16.8	10.8	25.7	Ref. 61, pg 101.
6	sec-Butyl alcohol	0.62	92.4	14.5	14.8	9.1	22.7	Ref. 61, pg 123
7	Isobutyl alcohol	**0.45**	92.8	15.1	16	5.7	22.7	Ref. 61, pg 101.
8	n-Butyl alcohol	0.33	91.9	15	15.4	10	23.7	Ref. 61, pg 101.
9	n-Butyl alcohol	0.33	91.5	16	15.8	5.7	23.1	Ref. 61, pg 123
10	tert-Amyl alcohol	0.39	109.6	13.8	12.4	10	21.1	Ref. 61, pg 101.
11	Ethylene glycol	2.2	56	17	26	11	32.9	(***)
12	Glycerol	1.8	73.2	9.3	31.4	15.4	36.2	Ref 61, pg130
13	Glycerol	1.8	73.2	17.4	27.2	11.3	36.1	(***)
14	Cyclohexyl alcohol	0.22	106	17.4	13.5	4.1	22.4	Ref. 61, pg 101.
15	Benzyl alcohol	0.09	103.7	14.7	15.6	12.2	24.6	Ref. 61, pg 123
16	Phenol	0.08	87.5	18	14.9	5.9	24.1	Ref. 61, pg 102
	Other cyclic compounds							
17	Aniline	0.08	92	19.4	10.2	5.1	22.5	Ref. 61, pg 123
18	Pyridine	0.09	80.9	17.6	7.7	10.1	21.7	Ref. 61, pg 135
19	1,4-Dioxane	0.64	85.7	19	7.4	1.8	20.5	Ref.61, pg 98
20	Butyrolactone	0.55	76.7	18.6	14	12.2	26.3	Ref. 61, pg 124
	Amides							
21	Formamide	1.9	39.8	17.2	19	26.2	36.6	Ref.61, pg 100
22	N-Ethylformamide	1	76.8				28.4	Ref.61, pg 253
23	N,N-Dimethylformamide	0.6	77	17.4	11.3	13.7	24.8	Ref.61, pg 100
24	Acetamide	1.1	60.8	17.3	22.4	18.7	33.92	Ref . 63
25	Acetamide	1.1	51				34.2	Ref.61, pg 268
26	N-Ethylacetamide	0.88	100.5				25.2	Ref.61, pg 253
27	N,N-Dimethylacetamide	0.6	93	16.8	10.2	11.5	22.7	Ref.61, pg 142
28	Propionamide	0.62	69.9	16.7	14.6	11.5	24.99	(***)
29	Propionamide	0.62	78.9	16.7	11.5	9.8	22.52	Ref. 63
30	Butyramide	0.46	95.4	16.9	12.3	13.7	24.99	(***)
31	Thioacetamide	0.62	68.3	17.5	20.2	20.6	33.74	(***)
	Ureas & others							
32	Urea	1	44.9	20.9	26.4	18.7	38.5	Ref. 61, pg 108
33	Thiourea	0.41	49.8	20	14.8	19.4	21.11	(***)
34	Acetonitrile	1.2	52.6	15.3	6.1	18	24.4	(***)
35	Acetonitrile	1.2	53	10.3	19.6	11.1	24.8	Ref. 61, pg 123
36	Water	NA	18	14.06	38.97	22.63	47.85	Ref. 61, pg (**)

(*)Adapted from Ref.[46]

(**) Average value of Hansen parameters for water calculated from Ref.[61] pgs.103,107, 115, 118, 137, 142, 288

(***) https://www.stevenabbott.co.uk/practical-solubility/hsp-basics.php

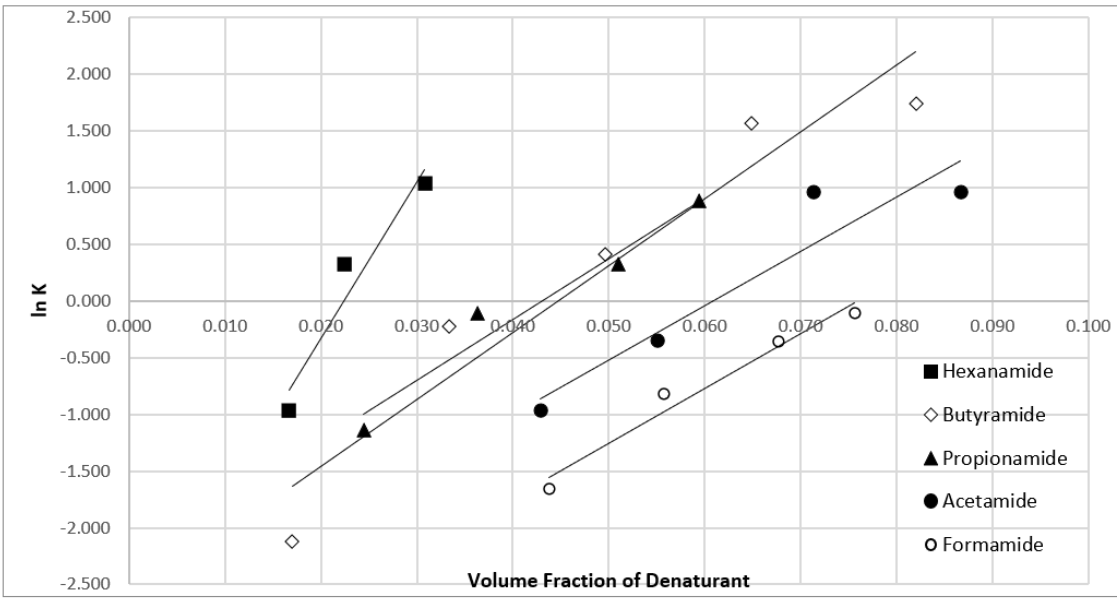

Fig 1a

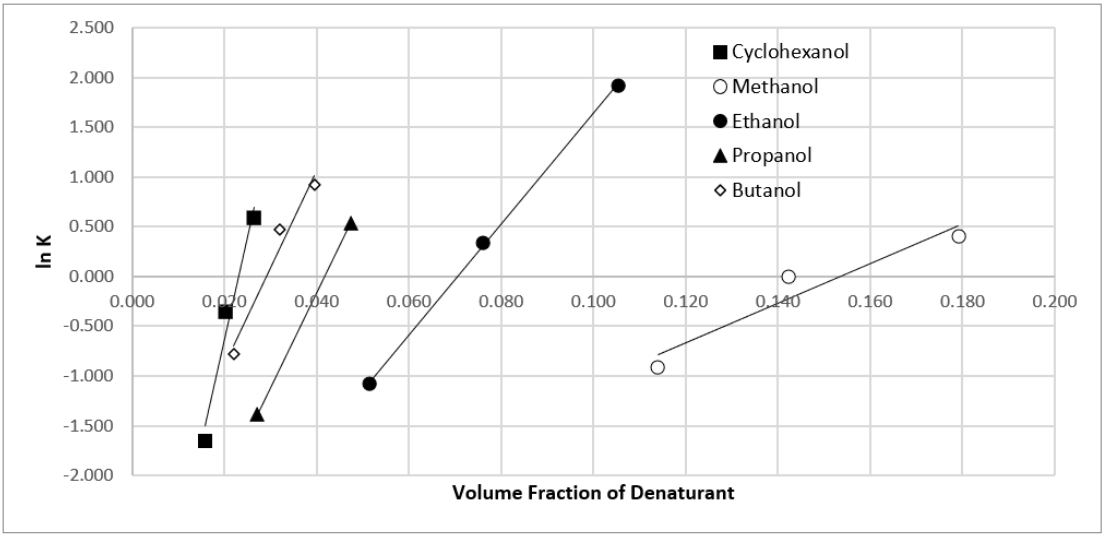

Fig 1b

Figure 1: Logarithmic plots of the ratio of denatured to native T4 bacteriophage DNA (ln K) as a function of the volume fraction (V_f) of denaturing agents in TRIS-EDTA buffer at 73 ° C, pH = 7.6. LnK and V_f values for Fig 1a and 1b were recalculated from experimental data of Levine.[46]

and minimize the error spread in Table 2.

Overall, we can conclude that the experimental data of Figure 1 confirm our theory describing the exothermic mechanism of the DNA chemical denaturation process. Note that in the opposite case (if a process were endothermic), the dependence of lnK vs V_f would be

Fig 2: Total and fractional enthalpies for solutions of chemicals at the concentration that is required to give 50% denaturation of T4 bacteriophage DNA at 346°K for three-component cohesion parameters

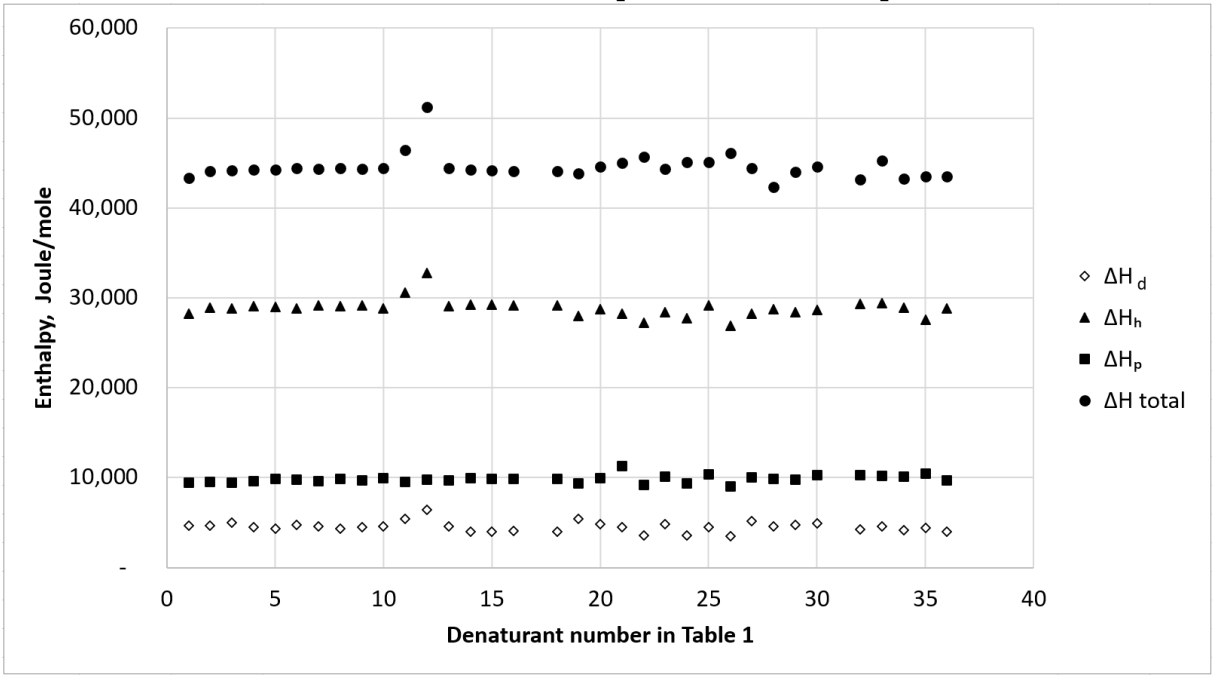

Figure 2: Total and partial enthalpies for denaturants of different structures described in Table 1.

Table 2
Comparison of the theoretical and experimental data for denaturation of T4 bacteriophage DNA in the presence of different denaturants in 0.05 M TRIS and 0.001 M EDTA buffer at 73°C, pH 7.6.

Denaturant	V [cm^3/mol]	Vr	Experimental "b" value (*)	Theoretical "b" value per expression 33.
Butyramide	84.4	4.69	59.3	85.8
Propionamide	78.9	4.38	57.7	63.6
Acetamide	51	2.83	43.8	58.7
Formamide	39.8	2.21	52.2	40.9
Cyclohexanol	108.2	6.01	212.1	111.2
Butanol	91.9	5.11	96.9	91.4
Propanol	75.2	4.18	94.4	65.6
Ethanol	58.5	3.25	55.7	46.5
Methanol	40.7	2.26	20.3	28.0

(*) Experimental "b" values calculated from slopes of ln K vs. V_f (see Fig. 1 and Eq. 32)

opposite (the slope of this dependence is reversed). The chemical denaturation experiments do not support this scenario.

We defined $\left(\delta^2 V V_f\right)_{sol,T_m}$ as parameter L_i. Verification of Equation 30 and 31 can also be done by measurements of the term:

$$\left(\sum_{i=1}^{i=j} \delta_i^2 V_i V_{f_i}\right)_{sol,Tm} = \left(\sum_{i=1}^{i=j} L_i\right)_{sol,Tm} \tag{35}$$

from the right part of Eq. 31 keeping the left part of Eq. 30 constant.

Temperature constancy is an important condition for such experiments where the same type and DNA concentration are used for denaturation in different solvents. At the melting point, the parameter L_i will remain the same for both DNA and the solution.

The authors[46] measured the degree of denaturation of T4 bacteriophage with a constant concentration in solutions of different denaturants at constant temperature $T = 73°C$. Each of these solutions has four components: a denaturant (1), 0.05 M Tris buffer (2), 0.001M EDTA (3), and water (w). The expression 35 can be written accordingly as $L_1+L_2+L_3+L_w$. Because $(L_1 + L_w) >> (L_2 + L_3)$ expression 35 is simplified as:

$$(\delta_1^2 V_1 V_{f_1} + \delta_w^2 V_w V_{f_w})_{sol,Tm} = (L_1 + L_w)_{sol,Tm} = L \tag{36}$$

and L_2 and L_3 are negligible because of their very low volume fraction,V_f.

Equations 21 and 22 together with 36 give expressions for enthalpy ΔH using full and fractional Hansen parameters describing chemical denaturation of DNA at its melting temperature when $lnK = 0$:

$$-\Delta H = (\delta_1^2 V_1 V_{f_1} + \delta_w^2 V_w V_{f_w} + RT)_{T_m} \tag{37}$$

$$-\Delta H_h = (\delta_{h_1}^2 V_1 V_{f_1} + \delta_{h_w}^2 V_w V_{f_w} + RTF_h)_{T_m} \tag{38}$$

$$-\Delta H_d = (\delta_{d_1}^2 V_1 V_{f_1} + \delta_{d_w}^2 V_w V_{f_w} + RTF_d)_{T_m} \tag{39}$$

$$-\Delta H_p = (\delta_{p1}^2 V_1 V_{f_1} + \delta_{p_w}^2 V_w V_{f_w} + RTF_p)_{T_m} \tag{40}$$

where ΔH_d is the fraction of enthalpy related to dispersion or non-polar forces, ΔH_h is the fraction of enthalpy related to hydrogen bonding forces, and ΔH_p is the fraction of enthalpy related to polar forces. $F_h = \frac{L_h}{(L_d+L_h+L_p)}$, $F_d = \frac{L_d}{(L_d+L_h+L_p)}$, and $F_p = \frac{L_p}{(L_d+L_h+L_p)}$. Note that $F_d + F_h + F_p = 1$.

All data presented in Fig 2 corresponds to a constant temperature of experiments $T = T_m$ and according to Eq.17 must have constant ΔH_{Tm} values, which is shown in Fig 2.

The selection of the wide range of different denaturants with significant differences in physicochemical parameters such as δ (20.5 to 47.85), V (18 to 110 $cm^3/mole$), and V_f (0.01 to 0.14) do not change the constancy of ΔH values at $T = T_m$ demonstrated in Fig 2. This is the second proof of the correctness of Eqs.30 and 31 that validates the theory. We can conclude that the Hildebrand equation applies to the chemical denaturation process.

The average values for the total and fractional enthalpies for a solution at T_m equal the enthalpies of the T4 bacteriophage DNA. These averages are presented in Table 3. Based on these data, we calculated the fractions of the enthalpy for dispersion, polar, or hydrogen types of DNA bonding.

Table 3: Averages for total and fractional entropies and enthalpies for solutions of chemicals at the concentration that is required to give 50% denaturation of T4 bacteriophage DNA at 346°K for three-component cohesion parameters

Enthalpy for solubility parameters	(ΔH) for δ_d	(ΔH) for δ_h	(ΔH) for δ_p	(ΔH) for total δ
(ΔH), J/Mole (*)	6,670.5	28,106.2	11,350.0	42,038.0
% to enthalpy total	15.9%	66.9%	27.0%	100.0%
(ΔS), Jole/(mol ° K) (**)	19.28	81.23	32.80	121.50

(*) The enthalpy values are the averages from the data presented on Fig.2
(**) Entropy calculated from Eq. 17

Results show that for chemical denaturation of T4 bacteriophage DNA, the effect of hydrogen bonding is the dominant part of enthalpy (67%). Table 3 also indicates that

dispersion forces have the lowest influence on enthalpy (11%). This direct experimental data is opposite to the conclusions presented by A.Dragan, Crane-Robinson, and P.Privalov (see introduction,[33,52]) related to the thermostability of DNA in the absence of denaturants.

Their results[33,52] show that dispersion (apolar, Van der Waals) forces are the main portion of the enthalpy. These forces provide around 60% of Gibbs free energy for DNA denaturation. Estimation[63] of fractional DNA cohesion parameters for polyelectrolyte (DNA) as averages for four DNA bases gives δ_d=19.8, δ_h= 12.3, δ_p=12.2. Corresponding fractional δ^2 values are 392.04, 151.29, 148.84. These δ^2 values are proportional to the enthalpy of denaturation. Thus the fractional enthalpy of DNA denaturation equals ΔH_d= 57%, ΔH_h=22%, and ΔH_p=22% i.e. the main portion (57%) of the enthalpy of the DNA thermal denaturation process belongs to dispersion forces that correspond to the conclusion of authors.[33,52] However, calculating the cohesive parameters of the polyelectrolyte as an average from four DNA bases is unclear because it did not consider the role of phosphate and other polar groups in a polyelectrolyte.

The opposite observations discussed above about the role of dispersion and hydrogen forces in the DNA denaturation process prove the differences in chemical and thermal denaturation mechanisms.

Analysis of Eq 17 showed that the only component containing the entropic term in the equation for chemical denaturation is T_m. The parameter T_m is included in Eqs. 37, 39, 38, 40. This leads to the conclusion that the chemical DNA denaturation process has both an enthalpic and entropic nature (See Eq. 17.)

Different DNA structures bond differently, and their resistance to the denaturation process can be different than in the case of T4 bacteriophage DNA. Levine[46] studied the chemical denaturation of six different types of DNA (including T4 bacteriophage) and showed that the stabilities of these different DNA molecules against denaturation in the presence of urea or pyridine increases with increasing guanine (G) plus cytosine (C) content of the DNA. This phenomenon can be explained by comparison of corresponding enthalpy changes.

Yirong Mo[83] shows that the GC pair has a binding energy ($-25.4 kcal/mol$) that is twice the binding energy of the adenine (A) and thymine (T) pair (-12.4 kcal/mol). This is why these different DNA molecules respond differently toward chemical denaturation in the presence of urea or pyridine and why a higher denaturant concentration is needed to melt DNA with higher GC content. According to Eqs.37, 38, 39,40, an increase in V_f of denaturants leads to an increase in the denaturing power of the solution needed to achieve 50% of DNA denaturation.

Levine et al.[46] also studied the effect of the concentration of T4 bacteriophage DNA on the degree of its denaturation. The authors[46] show that a higher degree of DNA denaturation in 1.0 M urea at $346°K$ occurred in more dilute solutions for DNA. This observation fits the prediction based on analysis of Eq. 30. An increase in DNA concentration, V_f, in the second term on the right-hand side of Eq 30, leads to a decrease in the lnK term. Thus, observing the effect of DNA concentration on denaturation further confirms our theory.

3.3 DNA denaturation analysis using expanded cohesion parameters.

Applying fractional cohesion parameters to calculate the enthalpies of chemical denaturation revealed the forces affecting this process. We applied Hansen's concept of three-component fractional cohesive parameters to consider the influences of the dispersion or non-polar interaction, the hydrogen bonding, and the polar interaction in the analysis of the chemical denaturation of DNA.

Karger, Keller, Snyder, and Eon developed[84,75,85,86] a set of five-component fractional cohesive/solubility parameters: δ_d = dispersion, δ_o = dipole orientation, δ_i = dipole induction, δ_a = hydrogen bonding related to proton-donor or acid (a), δ_b = hydrogen bonding related to proton-acceptor or base (b), and δ = total cohesive or solubility parameter. Parameter δ_o is related to the orientation effect between two molecules with a permanent dipole moment. Parameters δ_a and δ_b are presented by authors[74,75,84–86] to define nonsymmetrical

electron-donor and electron-acceptor properties of two components (DNA and denaturant) with different roles. This issue has been explained in terms of Lewis acid-base cohesion parameters.[87]

The relationship among these parameters is the following:

$$\delta^2 = \delta_d^2 + \delta_o^2 + 2\delta_i\delta_d + 2\delta_a\delta_b \tag{41}$$

This equation shows fractional cohesion parameters representing the acting forces affecting a solubility process. The methods of the experimental determination for each of these parameters are described in reference[61] page 75. The expressions for the enthalpies of the DNA denaturation process for five-component cohesion parameters shown below have been derived similarly to Eqs. 37, 39, 38, 40 for three-component cohesion parameters. The equation 37 for total enthalpy value is identical for three and five-component cases.

$$-\Delta H_d = (\delta_{d_1}^2 V_1 V_{f_1} + \delta_{d_w}^2 V_w V_{f_w} + RTF_d')_{T_m} \tag{42}$$

$$-\Delta H_o = (\delta_{o1}^2 V_1 V_{f_1} + \delta_{ow}^2 V_w V_{f_w} + RTF_o')_{T_m} \tag{43}$$

$$-\Delta H_i = (\delta_{i_1}^2 V_1 V_{f_1} + \delta_{iw}^2 V_w V_{f_w} + RTF_i')_{T_m} \tag{44}$$

$$-\Delta H_a = (\delta_{a_1}^2 V_1 V_{f_1} + \delta_{aw}^2 V_w V_{f_w} + RTF_a')_{T_m} \tag{45}$$

$$-\Delta H_b = (\delta_{b_1}^2 V_1 V_{f_1} + \delta_{bw}^2 V_w V_{f_w} + RTF_b')_{T_m} \tag{46}$$

where $F_d' = \frac{L_d'}{(L_d'+L_o'+L_i'+L_a'+L_b')}$, $F_o' = \frac{L_o'}{(L_d'+L_o'+L_i'+L_a'+L_b')}$, $F_i' = \frac{L_i'}{(L_d'+L_o'+L_i'+L_a'+L_b')}$, $F_a' = \frac{L_a'}{(L_a'+L_o'+L_i'+L_a'+L_b')}$, and $F_b' = \frac{L_b'}{(L_d'+L_o'+L_i'+L_a'+L_b')}$. Note that $F_d' + F_o' + F_i' + F_a' + F_b' = 1$.

Expressions above for total and fractional enthalpies ΔH describe the chemical denaturation of DNA at its melting temperature when $lnK = 0$.

We again analyzed the T_4 bacteriophage DNA denaturation data of Levine, Gordon, and Jencks's,[46] who studied a broad spectrum of chemicals as denaturants. Table 4 contains the concentration of denaturants in moles per liter (M) that create 50% of DNA denaturation at constant temperature ($73°C$). Table 4 also contains available experimental data for total and fractional cohesion parameters and corresponding referrals. These results are presented in Fig 3.

Table 4: Denaturant concentration (M) giving 50% denaturation of T4 bacteriophage DNA in TRIS-EDTA buffer solution PH=7.6 at 73°C and five-component cohesion parameters for denaturants at 25°C

#	Denaturants	M (*) Mol/Liter	V cm^3/mol	Total δ	δ_d at 25 ° C	δ_o at 25 ° C	δ_i at 25 ° C	δ_a at 25 ° C	δ_b at 25 ° C	References for cohesion data
	Alcohols									
1	Methyl alcohol	3.5	40.7	29.6	12.7	10	1.6	17	17	Ref. 61, pg 76
2	Ethyl alcohol	1.2	58.5	26	13.9	7	1	14.1	14.1	Ref. 61, pg 76.
3	n-Propyl alcohol	0.54	75.2	25	14.9	6.7	4.5	4.8	23.5	Ref. 61, pg 77.
4	n-Propyl alcohol	0.54	75.2	24.5	14.7	5.3	0.8	12.9	12.9	Ref. 61, pg 76.
5	sec-Butyl alcohol	0.62	92.4	22.7	15.2	5.4	3.2	3.5	23.3	Ref. 61, pg 77.
6	Isobutyl alcohol	0.45	92.8	23.1	15	5.8	3.4	3.8	22.8	Ref. 61, pg 77.
7	n-Butyl alcohol	0.33	91.9	23.7	15.3	5.4	3.1	4.6	22.6	Ref. 61, pg 77.
8	Ethylene glycol	2.2	56	34.8	16.4	13.9	2.3	12.5	12.5	Ref. 61, pg 76
9	Cyclohexyl alcohol	0.22	106	22.7	17.3	5.4	2.9	2.1	21.2	Ref. 61, pg 77.
10	Phenol	0.08	92	24.7	19.4	4.7	0.8	19	4.7	Ref. 61, pg 76.
	Other cyclic compounds									
11	Pyridine	0.09	80.9	21.7	17.4	7.8	2.1		10	Ref. 61, pg 76.
12	1,4-Dioxane	0.64	85.7	20.7	16	10.6	2.1		9.4	Ref. 61, pg 76.
13	gamma-Butyrolactone	0.55	76.7	26.3	16.4	14.7	6.5			Ref. 61, pg 76.
	Amides									
14	N,N-Dimethylformamide	0.6	77	24.1	16.2	12.7	4.9		9.4	Ref. 61, pg 76.
15	N,N-Dimethylacetamide	0.6	92	22.1	16.8	9.6	3.3		9.2	Ref. 61, pg 76.
	Others									
16	Acetonitrile	1.2	53	24.8	13.3	16.8	5.7		7.8	Ref. 61, pg 76.
17	Water		18	47.9	12.9	31.4	20.8	34.1	22.3	Ref. 61, Pgs (**)

(*)Values of M adapted from Ref.[46] Lawrence Levine, Julius A. Gordon, and W. P. Jencks
(**)Average cohesion parameters for water calculated from Ref.,[61] pgs.76, 77

Even though there are significant differences in physicochemical parameters such as δ

Fig 3: Total and fractional enthalpies for solutions of chemicals at the concentration that is required to give 50% denaturation of T4 bacteriophage DNA at 346°K for five-component cohesion parameters

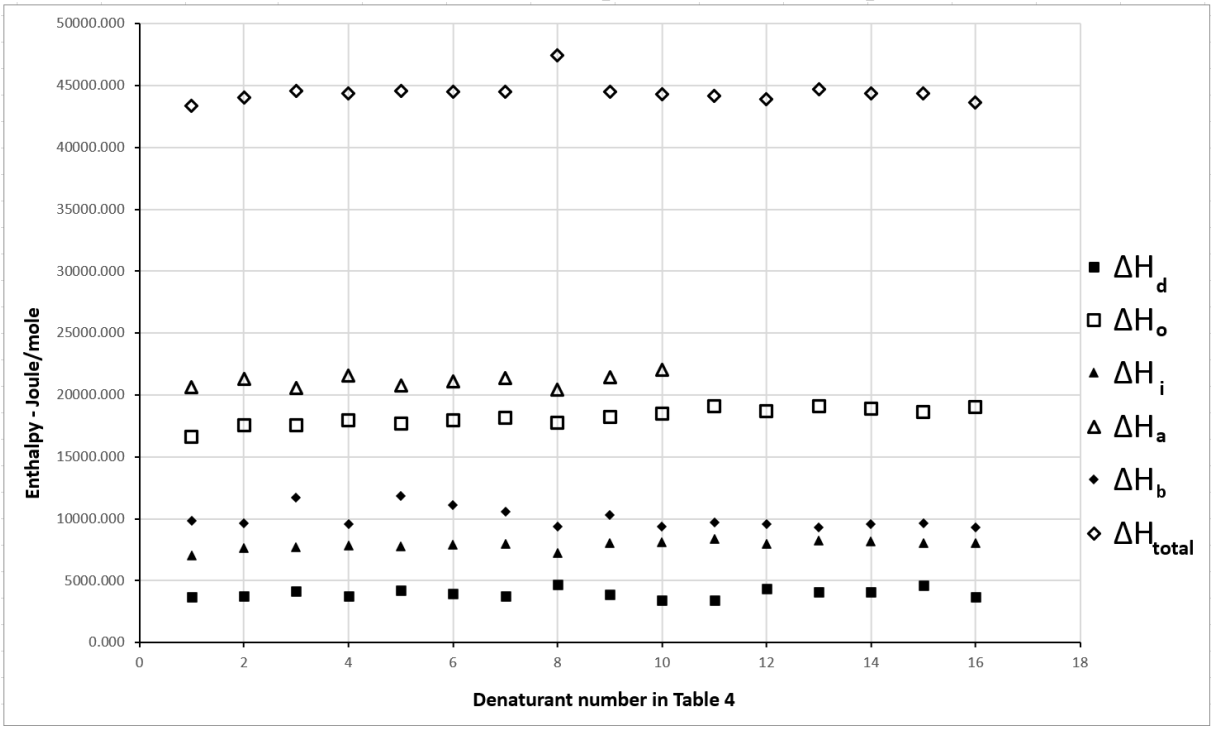

Figure 3: Total and fractional enthalpies for denaturants with different structures shown in Table 4.

(20.7 to 47.85), V (18 to 106 cm3/mole), and V_f (0.01 to 0.14), all total and fractional ΔH_{Tm} values stay constant. This again proves the correctness of Eq.31 that validates the theory for chemical denaturation.

The average values from Fig 3 of the total and each of the five fractional enthalpies for the denaturation process ΔH at $T = T_m$ are presented in Table 5. Based on this data, we calculated the fractions of the enthalpy responsible for specific mechanisms of DNA denaturation. Results show that for the chemical type of T4 bacteriophage DNA denaturation, melting is strongly related to the orientation effect (30%) as well as the disruption of hydrogen bonds in DNA according mainly to the proton-donor role of DNA (35%). Proton-acceptor role ΔH_b is significantly lower (16%).

Comparison of equations 22 and 41 for three-component and five-component cohesion

Table 5: Total and fractional entropies and enthalpies for the concentration of denaturant required to give 50% denaturation of T4 bacteriophage DNA at 346°K for five-component cohesion parameters

Enthalpy for solubility parameters	(ΔH) for total δ	(ΔH) for δ_d	(ΔH) for δ_o	(ΔH) for δ_i	(ΔH) for δ_a	(ΔH) for δ_b
(ΔH), Joule/Mole (*)	44,447.51	3,974.27	18,209.81	7,873.88	21,114.92	10,025.11
%		6%	30%	13%	35%	16%
(ΔS), Joule/(mol ° K) (**)	128.46	11.49	52.63	22.76	61.03	28.97

(*)The enthalpy values are the averages from the data presented in Fig.3
(**) Entropy at equilibrium in the system calculated as $\Delta S = \Delta H/T_m$

parameters leads to the conclusion that:

$$\delta_h^2 = 2\delta_a\delta_b \tag{47}$$

This equation and the data in Table 5 confirm our earlier conclusion from the analysis of Table 3 that the dominant role in the enthalpy of DNA denaturation is the disruption of hydrogen bonds. Five-component analysis reveals details of this mechanism related to nonsymmetrical electron-donor and electron-acceptor properties of two components (DNA and denaturant) with different roles.

Analysis of Table 5 shows the significant role of the orientation in the DNA denaturation process related to enthalpy. Sinanoglu and Abdulnur[43] show that DNA dipoles orienting the solvent dipoles are related to the entropic contribution to the solvent's free energy (ΔG). Thus, our data above and the data of authors[43] show that both the enthalpy and the entropy contribute to the orientation effect as part of the DNA denaturation process. This effect usually takes place as a result of two permanent dipole-dipole interactions. The connection of the orientation and induction cohesive components to such electrostatic parameters as dipole moment, polarizability, and ionization potential has been discussed by Gardon,[88,89] Keller, Karger, and Snyder[86] and Munafo, Buchman, Ho, and Kesselring.[90] Parameter δ_o of the five-component cohesion parameter set is related to δ_p from the three-component cohesion parameter set. Comparing equations 22 and 41 leads to the conclusion that

$$\delta_p^2 = \delta_o^2 + 2\delta_i\delta_d \tag{48}$$

The connection of the orientation and induction effects to the polar cohesion parameter has been discussed in the articles of[86],[88],[89].[90] The presence of the dispersion forces term in the polar cohesion parameter has historical roots. The polar-nonpolar solvent interaction had been studied mainly by Prauznitz and co-workers[68–71] during the development of an expression for the two-component cohesion parameter (before Hansen developed his three-component system) where $(\delta_o^2)'$ is only used in Prauznitz's equation and is not equal to δ_o^2 in equations 51 and 52.

Weimer and Prausnitz[70] suggested incorporating the product of polar and non-polar components δ_d and $(\delta_o)'$ into the theory. They noted a possible induction mechanism of polar-nonpolar interaction during the collision between one carbon-carbon bond with a polar molecule. This interaction is possible due to the known induction/polarizability of the carbon-carbon bond being attacked by a polar molecule. Another non-induction mechanism/role of orientation effect on the DNA renaturation process has been discussed by Privalov regarding base pairing and base stacking in the absence of solvents.[52] Both these processes required proper orientation of corresponding bases that were needed for the formation of hydrogen bonding. The incorporation of solvents should influence this orientational effect by a thermodynamical factor (as competitors for active sites on the bases) or by a geometrical (size) factor.

The five-component cohesion parameter theory,[86,90] and equation 41 expand previous knowledge related to the nature of partial cohesion parameters and allow us to obtain a deeper understanding of the physicochemical processes in DNA denaturation.

Overall, we can conclude that experimental data for DNA chemical denaturation has confirmed the theory developed in the present article and is based on the combination of Gibbs and Hildebrand's expanded thermodynamic approaches. This theory allows the calculation of both the enthalpy and the entropy at 50% DNA denaturation. The expression for the

entropy of this process at DNA melting temperature can be obtained by the combination of equations 17 and 26 :

$$(\Delta S)_{T_m} = \frac{\sum_{i=1}^{i=j} \delta_i^2 V_i V_{f_i}}{T_m} + R \tag{49}$$

3.4 Electrostatic repulsion forces participating in maintaining ds-DNA helix.

The presence of highly charged phosphate groups is the reason for electrostatic repulsion between two strands in dsDNA compensated by the attraction forces described above. All known fractional cohesion parameters are related to different attraction forces, and none define the contribution of repulsive (electrostatic) forces. So, until now, it has been unknown how to directly measure or even estimate the part of electrostatic repulsive forces responsible for maintaining the dsDNA helix. However, the stability of the dsDNA helix at equilibrium results from a balance between electrostatic repulsive forces and the sum of attractive forces defined by measurable or known fractional cohesion parameters described and evaluated earlier in the present article. Based on this balance, we can conclude that in the case of chemical denaturation, the total cohesion parameter for attraction forces is equal to and quantitatively describes electrostatic repulsion forces inside the dsDNA helix. This conclusion is valid for 50% DNA denaturation when, according to expressions 22, 25 and 31, cohesion parameters in solution correspond to similar parameters in DNA.

3.5 New method for revealing and evaluating of attraction and repulsion forces in DNA

The method uses the following steps:

- Select the targeted DNA or another system with controllable denaturation (object).

- Select several solutions with chemicals suitable for denaturing the object at the temperature needed for application. The cohesion parameters for selected chemicals should be

known.

- Measure the concentration of a denaturant needed for 50% of the object's denaturation at a constant temperature.

- Calculate total and fractional enthalpies for the object according to equations 35, 37, 38, 39, 40 and 42, 43, 44, 45, 46, or similarly modified equations (if there are more significant components in the solution).

- Use the results to reveal the influence of repulsive and different attractive forces at 50% denaturation of the object. Then, test different objects (DNA or other systems with controllable denaturation) using this method to find the one suitable for your needs.

3.6 Comparison of thermal and chemical types of DNA denaturation.

As shown above, the mechanisms of chemical and thermal denaturation processes are different. Thermal denaturation is an endothermic process, and chemical denaturation is an exothermic process. This endothermic type of denaturation can be demonstrated using recalculated experimental data of[46] as the temperature dependence of lnK with a negative slope of the Van't Hoff plot. The data is presented in Figs. 4 and 5.

Table 6 presents the enthalpy values for thermal denaturation calculated from the data of Figs 4 and 5. This table also contains the total enthalpy data for chemical DNA denaturation in solutions identical to those used for the thermal denaturation experiments.

The total enthalpies for chemical denaturation have been calculated using equation 37 according to experimental data of[46] and Hansen parameters recalculated for the temperature of the experiment.

Experiments for chemical denaturation and measurements have been conducted at constant temperatures.[46]

These data show that the enthalpy for thermal denaturation is positive (endothermic process), and the enthalpy for chemical denaturation is negative (exothermic process). Also, the absolute enthalpy values for DNA chemical denaturation are significantly lower than for

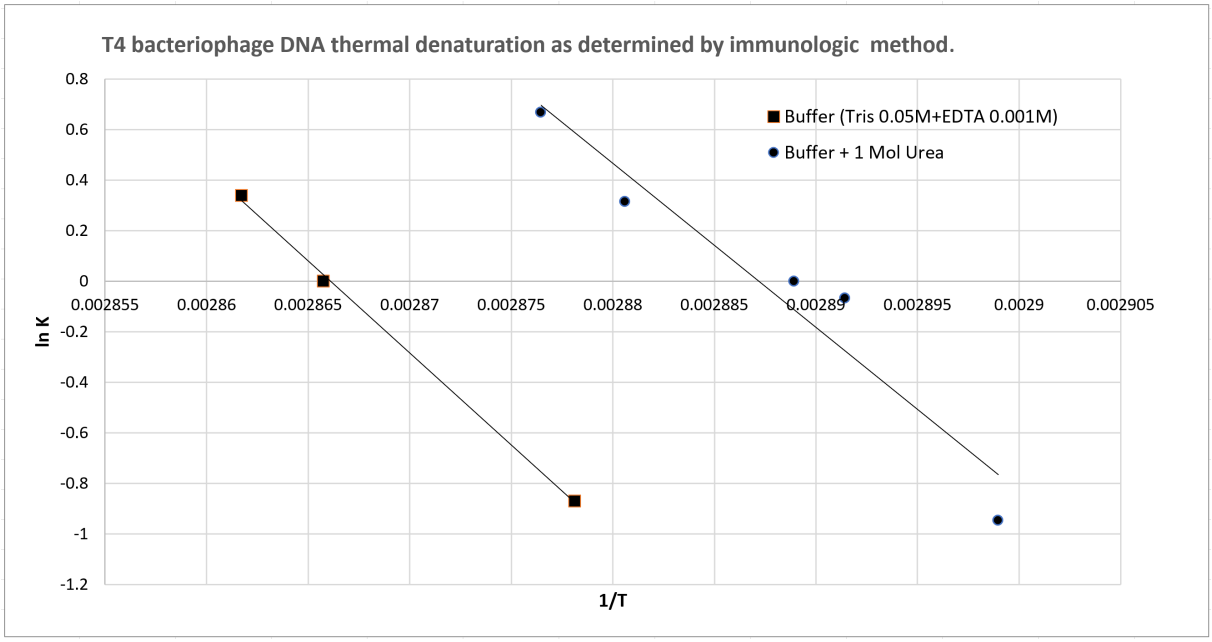

Figure 4: Thermal stability of DNA as determined by immunologic method. Denaturation has been performed in the presence and absence of Urea in Tris/EDTA buffer at 73°C. Recalculated from [46]

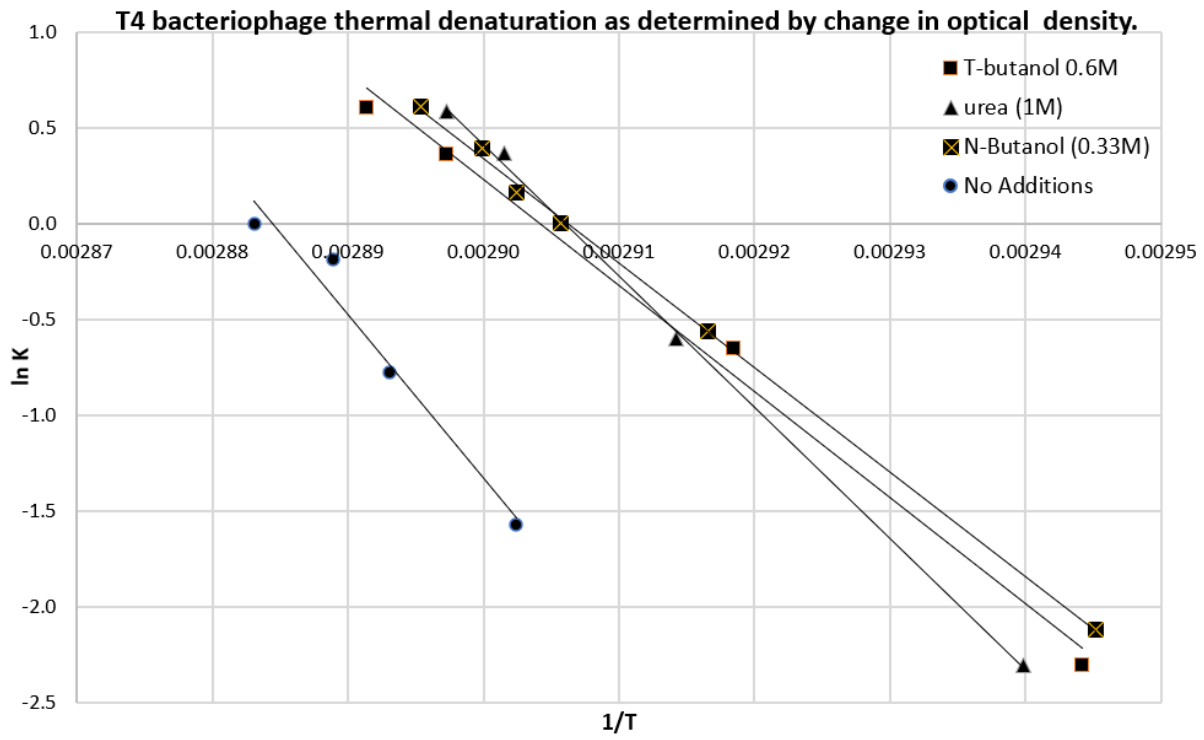

Figure 5: Thermal DNA stability as determined by change in optical density. Denaturation has been performed in the presence and absence of Urea, N-butanol, and T-butanol in Tris/EDTA buffer at 73°C. Recalculated from [46]

Table 6: Comparison of thermal and chemical denaturation of T4 bacteriophage DNA in the presence and absence of denaturants

Additives (*) to Tris +EDTA buffer	M for addatives (*)	Thermal denaturation process		Enthalpy (***) in chemical denaturation process at 346°K	Difference (T_m) chemical - (T_m) thermal
		Tm °K	Enthalpy (**)		
	mol/liter		Joule/mol	Joule/mol	°K
None	0	346.85	676,649	NA	NA
n-butanol	0.33	337.84	455,865	(43,980)	8.31
t-butanol	0.6	339.56	457,928	(44,058)	6.59
urea	1	337.84	564,285	(44,829)	8.31

(*) Value M is the concentration of denaturant required to give 50% denaturation of T4 bacteriophage DNA at $346°K$ in TRIS (0.05M) EDTA (0.001M) buffer. M values adapted from[46]

(**) The enthalpy calculated from the slopes on ln K=f(1/T) plots on Figs 4 and 5 multiplied by the universal gas constant.

(***) The total enthalpy calculated at $T_m = 346°K$ using Eq. 37 with experimental data for Vf and Hansen parameters.

the thermal denaturation process.

For thermal and chemical denaturation, there are differences in T_m. In the presence of urea or alcohol, the melting temperature for DNA thermal denaturation is $7°K$ to $8°K$ lower than for chemical denaturation in the same system. (Table 6). This confirms the conclusion that there is a difference in the mechanism of reaching 50% DNA denaturation in this process's thermal and chemical types.

Table 7 summarizes the major differences between thermal and chemical types of DNA denaturation.

The chemical denaturation process (at constant temperature) involves the replacement of initial bonds that kept DNA in double-stranded form, with the formation of new "DNA + denaturant" bonds with the higher energy of interaction leading to the separation of DNA strands with the formation of the random coils or single-stranded state. The enthalpy of the first stage of chemical denaturation (breaking the bonds inside DS DNA) is ΔH_{endo}. The enthalpy of the second stage of chemical denaturation (formation of new bonds with components of surrounding solution) is ΔH_{exo}. This process occurs spontaneously because the energy of interaction between active sites of DNA and components of the surrounding solution (including possible renaturation) should be higher or at least equal to the energy

Table 7
Differences between the Thermal and Chemical DNA denaturation processes.

Thermal denaturation (A)	**Chemical denaturation (B)**	**Notes**
The thermal denaturation of DNA is the endothermic process where the enthalpy is positive.	The chemical denaturation of DNA is the exothermic process where the enthalpy is negative.	(A)-See $\ln K$ vs. $1/T$ slopes, Figs 4 and 5, (B)-See the theory presented in this article with experimental verifications.
The Hildebrand equation does not apply to endothermal processes like thermal DNA denaturation.	The modified Hildebrand equation applies to exothermal processes such as chemical DNA denaturation.	See discussion in the section "DNA denaturation in one component liquid systems" related to expressions 21 and 20.
The value of enthalpy is significant: 450 – 650 K Joules/mol for T4 bacteriophage DNA	The value of enthalpy is small: (42 - 44) K Joules/mol for T4 bacteriophage DNA	See Table 6 for the A and B sections.
The melting temperature for thermal denaturation is lower than chemical: $7 - 8°K$ for T4 bacteriophage DNA. The melting temperature for chemical denaturation is higher than thermal: $7-8°K$ for T4 bacteriophage DNA	See Table 6 for the A and B sections.	
Hydrogen bonding/forces have only entropic, not enthalpic origin, and these forces are responsible for approximately 40% of Gibbs free energy of DNA denaturation .[33]	Hydrogen bonding has mainly enthalpic origin (61% of total enthalpy responsible for DNA denaturation). Disruption of hydrogen bonds is the dominant factor for denaturation	(A)-See introduction for references[32,33,52,53] (B)-See Tables 3 and 5.
Dispersion (apolar, Van der Waals) forces are the main portion of denaturation enthalpy. They provide around 60% of Gibbs free energy for DNA denaturation .[33]	The dispersion component of enthalpy has a small influence (9-15 %) on DNA denaturation.	(A)- See introduction for references[32,33,52,53] (B)- See Tables 3 and 5

of initial inter-DNA bonding involved in the denaturation process or $\Delta H_{exo} \geq \Delta H_{endo}$. (See Eq. 12) Thus, chemical denaturation is an exothermic process, negatively affecting the net enthalpy.

The thermal denaturation process involves breaking DNA bonds with dominant Van der Waals forces of an enthalpic nature.[33] We have the enthalpy-dominated hydrogen bond limiting denaturation in the case of DNA chemical denaturation at experimental conditions of authors.[46] Changes in DNA type and/or length and conditions of the experiment might lead to energetically different limiting steps in the chemical denaturation process related to the increased role of dispersion forces. This is the second possible explanation of differences in ΔH values for chemical and thermal processes.

Conclusions

1. We have developed a theory describing the chemical denaturation of DNA for low and medium denaturation degrees, including but not limited to 50% denaturation, as a reversible first-order reaction. The theory had no adjustable parameters; all parameters were known from independent data, and the theory was verified experimentally. This theory, with experimental data, shows the degree of influence of hydrogen bonding, dispersion, polar forces, proton donor/acceptor ratio, dipole induction, orientation parameter, and electrostatic interaction during DNA denaturation. The theory links the degree of DNA denaturation with the concentration of denaturants, Hildebrand, Hansen, KSE cohesion parameters, and temperature.

2. Thermal and chemical DNA denaturation have different thermodynamic parameters. The enthalpy for thermal denaturation is positive (endothermic process), and the enthalpy of DNA melting for chemical denaturation is negative (exothermic process). Experimental results show that the absolute enthalpy values for DNA chemical denaturation are significantly lower than in the thermal denaturation process. The melting temperature for DNA thermal

denaturation is lower than for chemical denaturation in the same system, indicating that the mechanism of reaching 50 % DNA denaturation thermally and chemically is different.

3. The analysis of the chemical DNA denaturation process using three-component fractional Hansen parameters shows that hydrogen bonding is the most significant part of the enthalpy of chemical denaturation for T4 bacteriophage DNA. The experimental data for the five fractional cohesion parameters show that the proton-donor effect is the dominant mechanism in hydrogen bonding changes during DNA denaturation. This effect's influence is two times larger than the proton-acceptor effect. Another essential factor for DNA denaturation is the orientational component, part of the polar cohesion parameter. We also suggested that the total cohesion parameter measured at 50% DNA chemical denaturation represents the electrostatic (repulsion) forces maintaining the DNA helix.

4. Theoretical and experimental results show that the Hildebrand, Hansen, and KSE equations are applicable and instrumental in studying DNA chemical denaturation.

5. We have developed a new method for revealing and estimating the degree of influence of repulsion and different attraction forces in DNA during its chemical denaturation. This method can be suitable for selecting DNA (or other systems with controllable denaturation) targeted for new applications.

Conflict of interest

The authors declare no conflict of interest.

Supporting Information

1. Total and Fractional Enthalpies for DNA denaturation by different chemical compositions (Excel)

2. Sizing effect of denaturants on chemical DNA denaturation (Excel)

References

(1) Chen, Y.-J.; Huang, X. DNA sequencing by denaturation: Principle and thermodynamic simulations. *Analytical biochemistry* **2009**, *384*, 170–179.

(2) Nie, Z. *DNA Nanotechnology for Cell Research: From Bioanalysis to Biomedicine*; John Wiley & Sons, 2024.

(3) Olave, B. DNA nanotechnology in ionic liquids and deep eutectic solvents. *Critical Reviews in Biotechnology* **2023**, 1–21.

(4) Keller, A.; Linko, V. Challenges and perspectives of DNA nanostructures in biomedicine. *Angewandte Chemie International Edition* **2020**, *59*, 15818–15833.

(5) Wang, Z.-G.; Ding, B. Engineering DNA self-assemblies as templates for functional nanostructures. *Accounts of chemical research* **2014**, *47*, 1654–1662.

(6) Jeon, H.; Nam, H.; Lee, J. B. Sustained release of minor-groove-binding antibiotic netropsin from calcium-coated groove-rich DNA particles. *Pharmaceutics* **2019**, *11*, 387.

(7) Chiorcea-Paquim, A.-M.; Oliveira-Brett, A. M. Electrochemistry of chemotherapeutic alkylating agents and their interaction with DNA. *Journal of pharmaceutical and biomedical analysis* **2023**, *222*, 115036.

(8) Jobling, M. A.; Gill, P. Encoded evidence: DNA in forensic analysis. *Nature Reviews Genetics* **2004**, *5*, 739–751.

(9) Zhu, Y.; Wu, J.; Zhou, Q. Functional DNA sensors integrated with nucleic acid signal amplification strategies for non-nucleic acid targets detection. *Biosensors and Bioelectronics* **2023**, 115282.

(10) Takinoue, M.; Suyama, A. Molecular reactions for a molecular memory based on hairpin DNA. *Chem-Bio Informatics Journal* **2004**, *4*, 93–100.

(11) Ussery, D. W. DNA denaturation. *Encyclopedia of genetics* **2001**, 550–553.

(12) Cheng, Y.-K.; Pettitt, B. M. Stabilities of double-and triple-strand helical nucleic acids. *Progress in biophysics and molecular biology* **1992**, *58*, 225–257.

(13) Nakano, S.-i.; Sugimoto, N. The structural stability and catalytic activity of DNA and RNA oligonucleotides in the presence of organic solvents. *Biophysical reviews* **2016**, *8*, 11–23.

(14) Hammouda, B. Insight into the denaturation transition of DNA. *International journal of biological macromolecules* **2009**, *45*, 532–534.

(15) Mura, M.; Carucci, C.; Marincola, F. C.; Monduzzi, M.; Parsons, D. F.; Salis, A. The melting curves of calf thymus-DNA are buffer specific. *Journal of Colloid and Interface Science* **2023**, *630*, 193–201.

(16) Owczarzy, R.; Moreira, B. G.; You, Y.; Behlke, M. A.; Walder, J. A. Predicting stability of DNA duplexes in solutions containing magnesium and monovalent cations. *Biochemistry* **2008**, *47*, 5336–5353.

(17) Muniz, M. I.; Bustos, A. H.; Slott, S.; Astakhova, K.; Weber, G. Cation valence dependence of hydrogen bond and stacking potentials in DNA mesoscopic models. *Biophysical Chemistry* **2023**, *294*, 106949.

(18) Matsarskaia, O.; Roosen-Runge, F.; Schreiber, F. Multivalent ions and biomolecules: Attempting a comprehensive perspective. *ChemPhysChem* **2020**, *21*, 1742–1767.

(19) Thomas, R. The denaturation of DNA. *Gene* **1993**, *135*, 77–79.

(20) Poland, D.; Scheraga, H. A. Occurrence of a phase transition in nucleic acid models. *The Journal of chemical physics* **1966**, *45*, 1464–1469.

(21) Poland, D.; Scheraga, H. A. Phase transitions in one dimension and the helix—coil transition in polyamino acids. *The Journal of chemical physics* **1966**, *45*, 1456–1463.

(22) Richard, C.; Guttmann, A. J. Poland–Scheraga models and the DNA denaturation transition. *Journal of statistical physics* **2004**, *115*, 925–947.

(23) Garel, T.; Monthus, C.; Orland, H. A simple model for DNA denaturation. *Europhysics Letters* **2001**, *55*, 132.

(24) Causo, M. S.; Coluzzi, B.; Grassberger, P. Simple model for the DNA denaturation transition. *Physical Review E* **2000**, *62*, 3958.

(25) Berger, Q.; Giacomin, G.; Khatib, M. Disorder and denaturation transition in the generalized Poland–Scheraga model. *Annales Henri Lebesgue* **2020**, *3*, 299–339.

(26) SantaLucia Jr, J. A unified view of polymer, dumbbell, and oligonucleotide DNA nearest-neighbor thermodynamics. Proc. of National Academy of Science USA. 1998; pp 1460–1465.

(27) Tinoco, I.; Uhlenbeck, O. C.; Levine, M. D. Estimation of secondary structure in ribonucleic acids. *Nature* **1971**, *230*, 362–367.

(28) SantaLucia Jr, J.; Hicks, D. The thermodynamics of DNA structural motifs. *Annu. Rev. Biophys. Biomol. Struct.* **2004**, *33*, 415–440.

(29) Sugimoto, N.; Nakano, S.-i.; Yoneyama, M.; Honda, K.-i. Improved thermodynamic parameters and helix initiation factor to predict stability of DNA duplexes. *Nucleic acids research* **1996**, *24*, 4501–4505.

(30) Petruska, J.; Goodman, M. F. Enthalpy-Entropy Compensation in DNA Melting Thermodynamics (). *Journal of Biological Chemistry* **1995**, *270*, 746–750.

(31) Privalov, P. L.; Crane-Robinson, C. Forces maintaining the DNA double helix. *European Biophysics Journal* **2020**, *49*, 315–321.

(32) Privalov, P. L.; Crane-Robinson, C. Translational entropy and DNA duplex stability. *Biophysical Journal* **2018**, *114*, 15–20.

(33) Dragan, A.; Privalov, P.; Crane-Robinson, C. Thermodynamics of DNA: heat capacity changes on duplex unfolding. *European Biophysics Journal* **2019**, *48*, 773–779.

(34) Kafri, Y.; Mukamel, D.; Peliti, L. Denaturation and unzipping of DNA: statistical mechanics of interacting loops. *Physica A: Statistical Mechanics and its Applications* **2002**, *306*, 39–50.

(35) Marenduzzo, D.; Bhattacharjee, S. M.; Maritan, A.; Orlandini, E.; Seno, F. Dynamical scaling of the DNA unzipping transition. *Physical review letters* **2001**, *88*, 028102.

(36) Wartell, R. M.; Benight, A. S. Thermal denaturation of DNA molecules: a comparison of theory with experiment. *Physics Reports* **1985**, *126*, 67–107.

(37) Blake, R. Cooperative lengths of DNA during melting. *Biopolymers: Original Research on Biomolecules* **1987**, *26*, 1063–1074.

(38) Khandelwal, G.; Bhyravabhotla, J. A phenomenological model for predicting melting temperatures of DNA sequences. *PloS one* **2010**, *5*, e12433.

(39) Lafontaine, I.; Lavery, R. Optimization of nucleic acid sequences. *Biophysical Journal* **2000**, *79*, 680–685.

(40) Delcourt, S. G.; Blake, R. Stacking energies in DNA. *Journal of Biological Chemistry* **1991**, *266*, 15160–15169.

(41) Breslauer, K. J.; Frank, R.; Blöcker, H.; Marky, L. A. Predicting DNA duplex stability from the base sequence. *Proceedings of the National Academy of Sciences* **1986**, *83*, 3746–3750.

(42) Schildkraut, C.; Lifson, S. Dependence of the melting temperature of DNA on salt concentration. *Biopolymers: Original Research on Biomolecules* **1965**, *3*, 195–208.

(43) Sínanoğlu, O.; Abdulnur, S. Hydrophobic stacking of bases and the solvent denaturation of DNA. *Photochemistry and Photobiology* **1964**, *3*, 333–342.

(44) Macedo, D.; Guedes, I.; Albuquerque, E. Thermal properties of a DNA denaturation with solvent interaction. *Physica A: Statistical Mechanics and its Applications* **2014**, *404*, 234–241.

(45) Mak, C. H. Unraveling base stacking driving forces in DNA. *The Journal of Physical Chemistry B* **2016**, *120*, 6010–6020.

(46) Levine, L.; Gordon, J. A.; Jencks, W. P. The Relationship of Structure to the Effectiveness of Denaturing Agents for Deoxyribonucleic Acid. *Biochemistry* **1963**, *2*, 31–36.

(47) Baldini, G.; Fu-Hua, H.; Varani, G.; Cordone, L.; Fornili, S.; Onori, G. DNA melting induced by alcohols: Role of the solvent properties. *Il Nuovo Cimento D* **1985**, *6*, 618–630.

(48) Cui, S.; Yu, J.; Kühner, F.; Schulten, K.; Gaub, H. E. Double-stranded DNA dissociates into single strands when dragged into a poor solvent. *Journal of the American Chemical Society* **2007**, *129*, 14710–14716.

(49) Mikhailenko, S. V.; Sergeyev, V. G.; Zinchenko, A. A.; Gallyamov, M. O.; Yaminsky, I. V.; Yoshikawa, K. Interplay between folding/unfolding and helix/coil transitions in giant DNA. *Biomacromolecules* **2000**, *1*, 597–603.

(50) Hammouda, B.; Worcester, D. The denaturation transition of DNA in mixed solvents. *Biophysical journal* **2006**, *91*, 2237–2242.

(51) Yakovchuk, P.; Protozanova, E.; Frank-Kamenetskii, M. D. Base-stacking and base-pairing contributions into thermal stability of the DNA double helix. *Nucleic acids research* **2006**, *34*, 564–574.

(52) Privalov, P. L. Physical basis of the DNA double helix. *Journal of Biophysics and Structural Biology* **2020**, *8*, 1–7.

(53) Crane-Robinson, C.; Privalov, P. Energetic basis of hydrogen bond formation in aqueous solution. *European Biophysics Journal* **2022**, *51*, 515–517.

(54) Levine, L.; Murakami, W.; Vunakis, H. V.; Grossman, L. Specific antibodies to thermally denatured deoxyribonucleic acid of phage T4. *Proceedings of the National Academy of Sciences* **1960**, *46*, 1038–1043.

(55) Xu, M.; Dai, T.; Wang, Y.; Yang, G. The incipient denaturation mechanism of DNA. *RSC advances* **2022**, *12*, 23356–23365.

(56) Chen, L.; Wang, Y.; Yang, G. Locally Denatured DNA Compaction by Divalent Cations. *The Journal of Physical Chemistry B* **2023**,

(57) Tongu, C.; Kenmotsu, T.; Yoshikawa, Y.; Zinchenko, A.; Chen, N.; Yoshikawa, K. Divalent cation shrinks DNA but inhibits its compaction with trivalent cation. *The Journal of Chemical Physics* **2016**, *144*.

(58) Bonner, G.; Klibanov, A. M. Structural stability of DNA in nonaqueous solvents. *Biotechnology and bioengineering* **2000**, *68*, 339–344.

(59) Blake, R.; Delcourt, S. G. Thermodynamic effects of formamide on DNA stability. *Nucleic acids research* **1996**, *24*, 2095–2103.

(60) Sturtevant, J. M.; Geiduschek, E. P. The heat of denaturation of DNA. *Journal of the American Chemical Society* **1958**, *80*, 2911–2911.

(61) Barton, A. F. *CRC handbook of solubility parameters and other cohesion parameters*; Routledge, 2017.

(62) van der Tol, J. J.; Vantomme, G.; Meijer, E. Solvent-Induced Pathway Complexity of Supramolecular Polymerization Unveiled Using the Hansen Solubility Parameters. *Journal of the American Chemical Society* **2023**, *145*, 17987–17994.

(63) CM, H. Hansen solubility parameters: a user's handbook. *Boca Raton, FL: CRC* **2007**,

(64) Bhamare, V. G.; Joshi, R. R.; Gangurde, M. S.; Pawar, V. V. Theoretical consideration of solubility by Hildebrand solubility approach. *World Journal of Advanced Research and Reviews* **2021**, *12*, 528–541.

(65) Louwerse, M. J.; Maldonado, A.; Rousseau, S.; Moreau-Masselon, C.; Roux, B.; Rothenberg, G. Revisiting Hansen solubility parameters by including thermodynamics. *ChemPhysChem* **2017**, *18*, 2999–3006.

(66) Jarvas, G.; Quellet, C.; Dallos, A. Estimation of Hansen solubility parameters using multivariate nonlinear QSPR modeling with COSMO screening charge density moments. *Fluid Phase Equilibria* **2011**, *309*, 8–14.

(67) Hildebrand, J.; Scott, R. Regular Solutions, Prentice-Hall. *Englewood Cliffs, NJ* **1962**,

(68) Hildebrand, J. H.; Prausnitz, J. M.; Scott, R. L. Regular and related solutions: the solubility of gases, liquids, and solids. *(Book)* **1970**,

(69) Blanks, R. F.; Prausnitz, J. Thermodynamics of polymer solubility in polar and nonpolar systems. *Industrial & Engineering Chemistry Fundamentals* **1964**, *3*, 1–8.

(70) Weimer, R.; Prausnitz, J. Screen extraction solvents this way. *Hydrocarbon Process* **1965**, *44*, 237.

(71) Kumar, R.; Prausnitz, J. Solvents in chemical technology. *Dack MRJ. Solutions and Solubilities, Part* **1975**, *1*, 259–326.

(72) Hansen, C. M. The Three Dimensional Solubility Parameter-Key to Paint Component Affinities: III; Independent Calculation of the Parameter Components. *Journal of Paint Technology* **1967**, *39*, 511–514.

(73) Hansen, C. *Macromolecular Solutions*; Elsevier, 1982; pp 1–9.

(74) Karger, B. L.; Snyder, L. R.; Eon, C. An expanded solubility parameter treatment for classification and use of chromatographic solvents and adsorbents: Parameters for dispersion, dipole and hydrogen bonding interactions. *Journal of Chromatography A* **1976**, *125*, 71–88.

(75) Karger, B. L.; Snyder, L. R.; Eon, C. Expanded solubility parameter treatment for classification and use of chromatographic solvents and adsorbents. *Analytical Chemistry* **1978**, *50*, 2126–2136.

(76) Kirkwood, J. G. The dielectric polarization of polar liquids. *The Journal of Chemical Physics* **1939**, *7*, 911–919.

(77) Hill, N. E. Dielectric properties and molecular behaviour. *(No Title)* **1969**,

(78) Mohan, T. M.; Sastry, S. S.; Murthy, V. Thermodynamic, dielectric and conformational studies on hydrogen bonded binary mixtures of propan-1-ol with methyl benzoate and ethyl benzoate. *Journal of solution chemistry* **2011**, *40*, 131–146.

(79) Miranda-Quintana, R. A.; Chen, L.; Smiatek, J. Insights into Hildebrand Solubility Parameters–Contributions from Cohesive Energies or Electrophilicity Densities? *ChemPhysChem* **2024**, *25*, e202300566.

(80) Panayiotou, C.; Mastrogeorgopoulos, S.; Aslanidou, D.; Avgidou, M.; Hatzimanikatis, V. Redefining solubility parameters: Bulk and surface properties from unified molecular descriptors. *The Journal of Chemical Thermodynamics* **2017**, *111*, 207–220.

(81) TEST, A. ACCU DYNE TEST™. *DIVERSIFIED Enterprises,[Online], available: https://www. accudynetest. com/solubility_ table. html*

(82) Abbott, S. Solubility science: principles and practice. *University of Leeds: Leeds, UK* **2017**, 109–110.

(83) Mo, Y. Probing the nature of hydrogen bonds in DNA base pairs. *Journal of molecular modeling* **2006**, *12*, 665–672.

(84) Karger, B. L.; Snyder, L. R.; Horvath, C. An introduction to separation science. *(Book)* **1973**,

(85) Keller, R. A.; Karger, B. L.; Snyder, L. R. Use of the solubility parameter in predicting chromatographic retention and eluotropic strength. *Gas Chromatography 1970* **1971**, 125.

(86) Keller, R. A.; Snyder, L. R. Relation between the solubility parameter and the liquid-solid solvent strength parameter. *Journal of Chromatographic Science* **1971**, *9*, 346–349.

(87) Wrona, P. K. On the correlations between empirical Lewis acid-base solvent parameters and the thermodynamic parameters of ion solvation. *Journal of Electroanalytical Chemistry and Interfacial Electrochemistry* **1980**, *108*, 153–167.

(88) Gardon, J. Cohesive-energy density. *Encyclopedia of polymer science and technology* **1965**, *3*, 833–862.

(89) Gardon, J. L. The influence of polarity upon the solubility parameter concept. *Journal of paint technology* **1966**, *38*, 43–57.

(90) Munafo, A.; Buchmann, M.; Nam-Tran, H.; Kesselring, U. W. Determination of the total and partial cohesion parameters of lipophilic liquids by gas-liquid chromatography and from molecular properties. *Journal of pharmaceutical sciences* **1988**, *77*, 169–174.